PILLARED CLAYS AS SUPERIOR CATALYSTS FOR SELECTIVE CATALYTIC REDUCTION OF NITRIC OXIDE

DE-FG22-96PC96206

FINAL TECHNICAL REPORT
September 1, 1996 - August 31, 2000

Submitted to

Attn: Ms. Dona G. Sheehan
FETC AAD Document Center
Federal Energy Technology Center
U.S. Department of Energy
MS 921-143
P. O. Box 10940
Pittsburgh, PA 15236-0940

by

Ralph T. Yang

Authors: R.Q. Long, N. Tharappiwattananon, W.B. Li and R. T. Yang
Department of Chemical Engineering
University of Michigan
Ann Arbor, MI 48109-2136

Table of Contents

Disclaimer

EXECUTIVE SUMMARY

Removal of NO_x ($NO + NO_2$) from exhaust gases is a challenging subject. V_2O_5-based catalysts are commercial catalysts for selective catalytic reduction (SCR) with NH_3 for stationary sources. However, for diesel and lean-burn gasoline engines in vehicles, hydrocarbons would be the preferred reducing agents over NH_3 because of the practical problems associated with the use of NH_3 (i.e., handling and slippage through the reactor). The noble-metal three-way catalysts are not effective under these conditions. The first catalyst found to be active for selective catalytic reduction of NO by hydrocarbons in the presence of excess oxygen was copper exchanged ZSM-5 and other zeolites, reported in 1990 by Iwamoto in Japan and Held et al. in Germany. Although Cu-ZSM-5 is very active and the most intensively studied catalyst, it suffers from severe deactivation in engine tests, mainly due to H_2O and SO_2. In this project, we found that ion-exchanged pillared clays and MCM-41 catalysts showed superior SCR activities of NO with hydrocarbon. All Cu^{2+}-exchanged pillared clays showed higher SCR activities than Cu-ZSM-5 reported in the literature. In particular, H_2O and SO_2 only slightly deactivated the SCR activity of Cu-TiO_2-PILC, whereas severe deactivation was observed for Cu-ZSM-5. Moreover, Pt/MCM-41 provided the highest specific NO reduction rates as compared with other Pt doped catalysts, i.e., Pt/Al_2O_3, Pt/SiO_2 and Pt/ZSM-5. The Pt/MCM-41 catalyst also showed a good stability in the presence of H_2O and SO_2. The results are described in detail in 4 chapters.

In Chapter 1, we report SCR of NO by C_2H_4 on ion-exchanged pillared clays, i.e., Cu-TiO_2-PILC, Cu-Al_2O_3-PILC, Cu-ZrO_2-PILC, Cu-Al_2O_3-Laponite, Fe-TiO_2-PILC, Ce-TiO_2-PILC, Co-TiO_2-PILC, Ag-TiO_2-PILC, Ga-TiO_2-PILC. Cu-TiO_2-PILC showed the highest activities at temperatures below 370 ^oC, while Cu-Al_2O_3-PILC was most active at above 370 ^oC, and both catalysts showed higher SCR activities than Cu-ZSM-5 reported in the literature. No detectable N_2O was formed by all of these catalysts. The catalytic activity increased with copper content until it reached 245% ion-exchange. In particular, H_2O and SO_2 only slightly deactivated the SCR activity of Cu-TiO_2-PILC, whereas severe deactivation was observed for Cu-ZSM-5. Moreover, the addition of 0.5 wt.% CeO_2 onto Cu-TiO_2-PILC increased the activities by about 10-30% while 1.0 wt.% of CeO_2 decreased the activity of Cu-TiO_2-PILC due to pore plugging. Subjecting the Cu-TiO_2-PILC catalysts to 5% H_2O and 50 ppm SO_2 at 700 ^oC for 2 h only slightly decreased its activity. TPR results showed that the overexchanged (245%) PILC sample contained Cu^{2+}, Cu^+ and CuO. The TPR temperatures for the Cu-TiO_2-PILC were substantially lower than that for Cu-ZSM-5, indicating easier redox on the PILC catalyst and hence higher SCR activity.

In chapter 2, SCR of NO_x by ethylene was investigated on copper ion and/or cerium ion-exchanged Al-MCM-41. Ce-Al-MCM-41 showed little activity, but Cu-Al-MCM-41 and cerium promoted Cu-Al-MCM-41 (i.e., Ce-Cu-Al-MCM-41) were found to be active in this reaction. Higher NO_x conversions to N_2 were obtained on the Ce-Cu-Al-MCM-41 as compared with Cu-Al-MCM-41. The maximum activity of Ce-Cu-Al-MCM-41 was close to that of Cu-ZSM-5; but the former had a wider temperature window. TPR results indicated that only isolated Cu^{2+} and Cu^+ ions were detected in the Cu^{2+}-exchanged Al-MCM-41 samples,

which may play an important role in the selective catalytic reduction of NO_x to N_2. After some cerium ions were introduced into Cu-Al-MCM-41, Cu^{2+} in the molecular sieve became more easily reducible by H_2. This may be related to the increase of catalytic activity of NO_x reduction by ethylene.

In chapter 3, we report SCR of NO by CH_4, C_2H_4, C_3H_6 and C_3H_8 on 0.5-5 wt% Pt/MCM-41 catalysts. The catalysts had high BET surface areas (> 900 m^2/g) and large pore volumes(> 1.00 cm^3/g). Platinum metal particles were detected in these catalysts at room temperature by XRD. A high activity for NO reduction was obtained when C_2H_4 or C_3H_6 was used as the reductant and the maximum NO reduction rate reached 4.3 mmol/g·h under the conditions of 1000 ppm NO, 1000 ppm C_3H_6, 2% of O_2 and He as balance; but no or little activity was found when CH_4 or C_3H_8 was used. This difference was related to the different nature of these hydrocarbons. The Pt/MCM-41 catalyst showed a good stability. H_2O and SO_2 did not cause deactivation of the catalyst. MCM-41 provided the highest specific NO reduction rates for Pt as compared with all other supports reported in the literature, i.e., Al_2O_3, SiO_2 and ZSM-5.

In chapter 4, we report Rh-exchanged Al-MCM-41 for SCR of NO by C_3H_6. It shows a high activity in converting NO to N_2 and N_2O at low temperatures. *In situ* FT-IR studies indicate that Rh-NO^+ species (1910-1898 cm^{-1}) is formed on the Rh-Al-MCM-41 catalyst in flowing NO/He, NO+O_2/He and NO+C_3H_6+O_2/He at 100-350 ^oC. This species is quite active in reacting with propylene and/or propylene adspecies (e.g., π-C_3H_5, polyene, etc.) at 250 ^oC in the presence/absence of oxygen, leading to the formation of the isocyanate species (Rh-NCO, at 2174 cm^{-1}), CO and CO_2. Rh-NCO is also detected under reaction conditions.

A possible reaction pathway for reduction of NO by C_3H_6 is proposed. In the SCR reaction, Rh-NO^+ and propylene adspecies react to generate the Rh-NCO species, then Rh-NCO reacts with O_2 , NO and NO_2 to produce N_2, N_2O and CO_2. Rh-NO^+ and Rh-NCO species are two main intermediates for the SCR reaction on Rh-Al-MCM-41 catalyst.

CHAPTER ONE

Ion Exchanged Pillared Clays for Selective Catalytic Reduction of NO by Ethylene in the Presence of Oxygen

Introduction

Selective catalytic reduction (SCR) of NO by NH_3 is presently performed with vanadia-based catalysts for flue gas applications [1]. Hydrocarbons would be the preferred reducing agents over NH_3 because of the practical problems associated with the use of NH_3 (i.e., handling and slippage through the reactor). SCR of NO by hydrocarbon can also find important applications for lean-burn (i.e., O_2-rich) gasoline and diesel engines where the noble-metal three-way catalysts are not effective in the presence of excess oxygen [2-4].

The first catalysts found to be active for SCR of NO by hydrocarbons in the presence of oxygen were Cu^{2+} ion-exchanged ZSM-5 and other zeolites, reported in 1990 by Iwamoto [5] and Held et al. [6] and in early patents cited in [7]. Reports on a large number of catalysts for this reaction have appeared since 1990. The majority of these catalysts are ion-exchanged zeolites, including H^+ forms. Metal oxides supported on alumina have also been studied, but are less active. Noble metals and their ion-exchanged forms have also been studied widely. The early (1990-1992) literature on the subject, primarily by Japanese researchers, has been reviewed by Iwamoto and Mizuno [6] and will not be repeated here. The most active catalysts include: Cu-ZSM-5 [3, 5-20]. Co-ZSM-5 [18, 21-28], Cu-Na-ZSM-5 [29], Ce-ZSM-5 [30, 31], Fe-ZSM-5 [32-34], Pt-ZSM-5 [35], Pd-ZSM-5 [36], Mn-ZSM-5 [37], Ga-ZSM-5 [38, 39], Cu-Zr-O and Cu-Ga-O [40, 41], Ag/Al_2O_3 [42, 43], Pt/Al_2O_3 [44], Pd/TiO_2 [45, 46], CuO/Al_2O_3 [47, 48], Co/Al_2O_3 [49], Supported Au [50], La_2O_3 [51] and Ga/ZrO_x [52]. Reviews on the subject are available [2, 53, 54].

It is known that the SCR reactions, both by NH_3 and by hydrocarbons, are limited by the pore diffusion rates (for NH_3 SCR, see for example, 55 and 56; for HC SCR, [3, 13, 57,

58]). From the overall rates, it is not a trivial task to calculate the intrinsic rates and the pore diffusivities [56]. Pore diffusion limitation also plays a significant role in the SCR by pillared clay catalysts, to be discussed below.

Pillared interlayered clays (PILCs) or pillared clays are two-dimensional zeolite- like materials prepared by exchanging the charge-compensating cations between the clay layers with large inorganic hydroxycations, which are polymeric or oligomeric hydroxy metal cations formed by hydrolysis of metal oxides or salts. Upon heating, the metal hydroxy cations undergo dehydration and dehydroxylation, forming stable metal oxide clusters which act as pillars keeping the silicate layers separated, creating interlayer space of molecular dimensions. Since pillared clays have a number of attractive features such as porosity, high thermal stability and exchangeable cations, they have been widely studied as catalysts and adsorbents [59]. More specifically, the PILC based catalysts have been found to be excellent and H_2O/SO_2 resistant catalysts for the SCR reactions by NH_3 and by hydrocarbons [60]. The PILCs alone showed NH_3 SCR activities [61], with Fe_2O_3-PILC exhibiting the highest activities [62]. Using TiO_2-PILC as a support, a 3/1 (molar ratio) of Fe_2O_3/Cr_2O_3 (total 10% wt.) showed an NH_3 SCR activity twice as high as that of the commercial V_2O_5/TiO_2 catalyst [63]. For HC SCR, Cu-ion exchanged PILC yielded activities higher than that of Cu-ZSM-5; and more significantly, its activity was only slightly decreased by H_2O and SO_2 [57, 58]. This is significantly different from Cu-ZSM-5 which is severed deactivated by H_2O/SO_2. An FTIR study of the reaction showed that the surface species were mainly bidentate nitrate, monodentate nitrate and nitro species bonded to Cu^{2+} [64]. Cu-exchanged pillared clay has also been found to be active for NH_3 SCR [65]. Ion-exchanged Al_2O_3-PILC has shown high activities for glycol ether production from epoxide and ethanol [66], and oxidative dehydrogenerations of propane [67].

In this work, $A1_2O_3$-PILC (Al-PILC), ZrO_2-PILC (Zr-PILC) and TiO_2-PILC (Ti-PILC), were synthesized. Cu-Ti-PILC, Cu-Al-PILC and, Cu-Zr-PILC were studied for SCR of NO with ethylene as the reductant. (In addition, a synthetic clay, Laponite, was also included, as Cu-Al_2O_3-pillared Laponite.) The SCR activities were first investigated by comparing directly with that of Cu-ZSM-5. Effects of water vapor and sulfur dioxide on catalytic activity were examined. The effect of the promoter (Ce_2O_3) was studied on Cu-Ti-PILC. The SCR activities of pillared clays with a number of other cations (Fe-Ti-PILC, Ce-Ti-PILC, Co-Ti-PILC, Ag-Ti-PILC and Ga-Ti-PILC) were also studied.

2. Experimental

2.1. Syntheses of Pillared Interlayered Clays (PILCs)

The first step in PILC synthesis is preparation and aging of the pillaring solution to form oligomers. The pillaring solution undergoes hydrolysis, polymerization, and complexation with anion in the solution [68, 69]. The hydrolysis conditions, i.e., temperature, pH, and aging time, are important to the formation of PILC. The next step is intercalation of the small cations between the clay layers with the oligomers. This is done by preparing a slurry consisting of a suspension of the clay in deionized water, oligomeric solution, and HCl and NaOH used for pH adjustment. The oligomeric solution is added dropwise to the clay suspension with vigorous stirring. Slow addition of the solution helps in the formation of uniform pillared clays. After completion of intercalation, the sample is separated from the liquid phase by centrifligation or vacuum filtration. The final step is drying and calcination.

2.1.1. TiO_2-PILC (Ti-PILC) synthesis

The starting clay was a purified montmorillonite, as purified-grade bentonite powder

from Fisher Company, which had a particle size of 2~m or less. This bentonite (originating in Wyoming) had a cation exchange capacity (CEC) of 76 meq/100g clay. The pillaring solution of partially hydrolyzed Ti-polycations was prepared by first adding $TiCl_4$ into 1 M HCl solution. The mixture was then diluted by slowly adding deionized water with rigorously stirring to reach a final Ti concentration of 0.82 M and a final HCl concentration of 0.11 M [70]. The solution was aged for 24 hr at room temperature. A 4g amount of starting clay was dispersed in 1 L of deionized water by 24 hr prolonged stirring [63]. The pillaring solution was slowly added with vigorous stirring into the suspension of clay until the amount of pillaring solution reached that required to obtain a Ti/Clay ratio of 10 mM of Ti/g clay. The intercalation step took 24 hr and subsequently the mixture was separated by vacuum filtration or centrifligation and washed with deionized water until the liquid phase was free of chloride ions by silver nitrate test. The sample was dried at 120°C for 12 hr. and calcined at 300°C for 12 hr.

2.1.2. ZrO_2-PILC (Zr-PILC) synthesis

The starting materials for preparation of zirconium pillared clay were the purify grade bentonite 'from Fisher and zirconyl chloride ($ZrOCl_2 \bullet 8H_2O$) as the pillaring agent. The oligomeric solution was prepared from $ZrOCl_2 \sim 8H_2O$ by dissolving the salt in deionized water to obtain a 0.1 M solution. The solution was aged at room temperature at pH of 1.3 for three days. The main intercalating species was the tetramer, $[Zr_4(OH)1_4(H_20)10]^{2+}$ [71]. The pillaring solution, normally 50 ml was added dropwise to 1 g clay suspension while vigorous stirring was maintained to get pillaring stoichiometry at 5 mmol of Zr/l g clay. The intercalation was conducted at room temperature for three days. The sample was then separated and washed by vacuum filtration until no chloride ions remained. Finally the sample was dried and calcined in air at 350°C for 12 hr.

2.1.3. $A1_2O_3$-PILC (Al-PILC) synthesis

The starting clay was the same purified grade bentonite. The aluminum hydroxy-oligomeric solution was prepared by slowly adding 0.1 M NaOH into 0.2 M $AlCl_3$ solution under constant stirring until reaching a OH/Al ratio of 2.0. The stirring during the addition of NaOH was necessary in order to prevent local accumulation of hydroxyl ions, which invariably produced precipitation of $Al(OH)_3$ [72]. The oligomeric solution was aged for a day at pH 4.2 with the main intercalation species, $[Al_{13}0_4(OH)_{24}(H_2O)_{12}]^{7+}$ [73]. A suspension containing 1% bentonite in deionized water was mixed with the oligomeric solution at an Al/OH ratio of 10 mmol AI/g clay. The mixture was allowed to react at room temperature for 24 hr before being subjected to vacuum filtration and washing until free of chloride ions. The sample was then dried and calcined up to 3500C for 12 hr.

2.2. Catalyst Preparation

2.2.1. Cu^{2+}-exchanged Ti-PILC (Cu-Ti-PILC), Cu^{2+}-exchanged Zr-PILC (Cu-Zr-PILC) and Cu^{2+}-exchanged Al-PILC (Cu-Al-PILC)

One gram of the obtained pillared bentonite was added to 100 ri' of 0.02 M copper nitrate solution. The mixture was stirred for 24 hr at 50°C. The pH of the starting solution was adjusted to 6.0 by adding a proper amount of ammonia solution. The ion exchange product was collected by filtration or centrifugation followed by washing with deionized water five times. The obtained solid sample was first dried at 120°C in air for 12 hr, then the sample was further calcined at 400°C in air. The sample was finally ground to collect the 100-140 mesh fraction. After this pretreatment, the sample was ready for further experiments.

2.2.2. Cu2+-exchanged Al_2O_3-pillared laponite (Cu-Al-Lapo)

Delaminated Al_2O_3-pillared laponite was obtained from Laporte Industries, Ltd (CEC = 94 meq/l00g clay). Laponite is a synthetic hectorite. Prior to use, it was suspended as 1 wt% slurry and wash with dilute NH_4NO_3 solution to remove impurities and metal ions. After filtration, the residue was dried at 120°C then it was again suspended as 1% slurry. The slurry was added with 10 mL of 1.0 M $Cu(NO)_3)_2$ solution with constant stirring. The pH of the mixture was adjusted to 5.5 by using ammonia solution. The solution then kept at 50°C for 24 hr. Subsequently, the sample was filtrated and washed thoroughly with deionized water five times. The residue was dried and calcined at 400°C for 12 hr.

2.2.3. Cu^{2+}-exchanged ZSM-5 (Cu-ZSM-5)

The Cu^{2+}-exchanged ZSM-5 was prepared by mixing the ZSM-5 sample with an aqueous solution of cupric nitrate. The Si/A1 ratio in the ZSM-5 was 40. Before the ion exchange, the ZSM-5 was washed in 0.01 M $NaNO_3$ solution. After washing, 2 g of ZSM-5 was added to 100 mL of 0.01 M $Cu(NO)_3)_2$, with constant stirring for 24 hr. The sample was collected after the resulting suspension was filtered, washed, dried and calcined at 400°C for 12 hr. The sample pretreatment was also made before the sample was ready for catalytic experiments.

2.2.4. Cu-doped-Ti-PILC (Cu/Ti-PILC)

Copper was introduced into Ti-PILC by incipient wetness impregnation by using $Cu(NO)_3)_2$ solution. The copper amount was 5.9 wt%. The Cu-doped-Ti-PILC was dried at 120°C for 12 hr and calcined at 400°C for 12 hr.

2.2.5. Ce-promoted-Cu-Ti-PILC (Ce/Cu-PILC)

Ce_2O_3 0.5-1.0 wt% was doped into Cu-Ti-PILC (Cu 5.9 wt%) by incipient wetness impregnation by using $Ce(\sim O)_3)_3$ solution. The sample was then dried and calcined at 400°C for 12 hr.

2.2.6. Other cation-exchanged-Ti-PILC (Fe-Ti-PILC, Ce-Ti-PILC, Co-Ti-PILC, Ag-Ti-PILC and Ga-Ti-PILC)

The catalysts were prepared by ion exchange of Ti-PILC with aqueous solutions of $Fe(NO)_3)_3$, $Ce(NO)_3)_3$, $Co(NO)_3)_3$, $AgNO)_3$, and $Ga(NO)_3)_3$. The standard ion exchange procedure was used. Each gram of Ti-PILC was added to each 100 mL of 0.02M nitrate solution. The mixture was stirred for 24 hr at room temperature. The ion-exchanged product was collected by filtration and washed with deionized water five times. The ion exchange was repeated three times. Then the final product was dried at 120°C for 12 hr and calcined at 400°C for 12 hr. The catalysts were Fe-Ti-PILC (Fe 6.8 wt%), Ce-Ti-PILC (Ce 1.0 wt%), Co-Ti-PILC (Co 0.5 wt%), Ag-Ti-PILC (Ag 5.7 wt%), and Ga-Ti- PILC(Ga 5.6 wt%

2.3. Characterization

The chemical analyses were performed by neutron activation analyses.

2.3.1. BET surface area

A Micromeritics ASAP 2010 micropore size analyzer was used to measure the N_2 adsorption isotherm at liquid N_2 temperature (77K). BET surface areas and pore volumes were calculated from the isotherms.

2.3.2 X-ray diffraction

A Rigaku 12 kW rotating anode x-ray diffraction unit with Cu K~ was used to measure the x-ray diffraction patterns of the samples.

2.4. Catalytic Activity Measurement

The scheme of reaction apparatus is shown in Fig. 1. The test reactor consisted of a quartz tube containing a quartz fritted support. The catalyst sample was placed on the frit, and covered with a layer of glass wool. The heating element was a coiled Nichrome wire. The reactor temperature was controlled by an Omega CN-20 10 programmable temperature controller. The flue gas was simulated by blending gaseous reactants. Two sets of flow meters were used to control the flow rates of reactants. High flow rates (i.e., He, NO/He or C_2H_4/He) were controlled by rotameters, whereas the low flow rates (i.e., O_2, SO_2 /He) were controller by mass flow meters (FC-260 Tylan). The pre-mixed gases (1.0% NO in He, 1.0% SO_2 in He, and 1.0% C_2H_4 in He) were supplied by Matheson. Water vapor was generated by passing helium gas through a gas-wash bottle containing deionized water. The typical reactant gas composition was as follows: 1,000 ppm of NO; 1,000 ppm of C_2H_4; 2% of oxygen; 500 ppm of SO_2 (when used); 5% water vapor (when used), and balance of He. The total flow rate was 250 cc/mm. (ambient conditions). The catalyst size fraction was 100-140 mesh, and *0.5* g was used in typical experiment. The NO concentration was continuously monitored by a chemiluminescent NO/NOx analyzer (Thermo Electron Corporation, model 10). A Shimadzu GC model 1 4A was used to analyze the concentrations of N_2 and N_20 in the product stream. The analytical system had two capillary columns: a Poropak Q column used to analyze N_20 and $C0_2$, and a molecular sieve SA used to analyze N_2, O_2, CO and NO.

3. Results and Discussions

3.1. Surface Areas and Nitrogen Adsorption

The BET surface areas and the pore volumes of all pillared clay samples are summarized in Table 1. According to the Brunauer, Deming, Deming, and Teller (BDDT) classification, the N_2 adsorption isotherms at 77 K for Ti-PILC, Al-PILC and Zr-PILC showed type IV isotherm shape indicating the presence of both micropores and mesopores. The large surface areas and pore volumes were the results of successful pillaring. The Ti-PILC had a larger surface area and pore volume than Al-PILC and Zr-PILC. The Ti-PILC also had a surface area in the same range with Al-Laponite from Laporte Industries.

3.2. X-ray Diffraction Study

X-ray diffraction patterns (XRD) of the starting clay (Fisher bentonite), Al-PILC, Zr-PILC, Ti-PILC and Al-Laponite are measured. Generally, XRD patterns of smectite clays show basal (001) reflection and two dimensional hk reflection only. Other hkl reflections are usually not observed.

The pattern of Fisher bentonite was recorded after the sample was calcined at 350°C for 12 hr. The 20 angle of the (001) reflection was 8.95° which corresponded to a d-spacing of 9.87 A. The corresponding 2θ angles of the (hk) two-dimensional peaks were at 19.6° and 35°. These hk two-dimensioinal diffraction arise from the diffraction of the random stacking of layers. The diffraction at 2θ of 19.6° is the summation of hk indices of (02) and (11) and the diffraction of 35° is the summation of hk indices of (13) and (20). The peak at 2θ of 26.5° is a reflection of the quartz impurity.

In the PILC samples, the d_{001} spacing were 18.98 and 17.83 A for Zr-PILC and Al-PILC respectively. The free interlayer spacing in these pillared clays were obtained by subtracting 9.6 A, the thickness of the aluminosilicate layer. The resulting free interlayer spacings are shown in Table 1.

3.3. Comparison of Activities of Cu-Ti-PILC, Cu-Al-PILC, Cu-Zr-PILC and Cu-ZSM-5

In Fig. 2, the catalytic behaviors for SCR of NO by ethylene in the presence of oxygen of Cu-Ti-PILC, Cu-Zr-PILC, Cu-Al-PILC and Cu-Al-Laponite are compared with the catalytic behavior of Cu-ZSM-5, which is the most extensively studied catalyst for this reaction. These five catalysts were studied under identical reaction conditions. It is clear that the catalytic activity increased with increasing temperature, reaching a maximum NO conversion, and then decreased at higher temperatures. The temperature at the maximum conversion had the following values: 300°C for Cu-Ti-PILC, 3500C for Cu-Al-PILC, Cu-Zr-PILC and Cu-ZSM-5, and 400°C for Cu-Al-Laponite. The peaking of NO conversion at a certain temperature for SCR is the result of two competing reactions: NO reduction by hydrocarbon and oxidation of hydrocarbon by oxygen. The oxidation of hydrocarbon, which reduced the amount of reductant, had a stronger effect in the higher temperature range.

The degrees of Cu ion-exchange are summarized in Table 2. The copper content was obtained by neutron activation analysis. The ion-exchange level of Cu-ZSM-5 was calculated by (2 x number of copper ions)/(number of aluminum atoms) x 100. The ion-exchange levels of Cu-PILC were calculated by (2 x number of copper ions)/(CEC) x 100. From the percentage of copper loading in Table 2, the catalysts were over-exchanged. The over-exchanged catalysts resulted from the presence of not only Cu^{2+} but also from the presence of Cu^{+} and CuO. The results in Fig. 2 show that Cu-Ti-PILC is more active than Cu-ZSM-5 and the two other Cu-exchanged pillared clays (Cu-Al-PILC and Cu-Zr-PILC). The physical characterization data in Table 1 show that Ti-PILC had a higher surface area which could provide more accessible active sites. Figure 2 also shows that Cu-Al-Laponite had the highest SCR activity in the higher temperature range.

3.4. Effect of Copper Loading of Cu-Ti-PILCs on SCR of NO

Six samples of Cu-Ti-PILCs were used to study the effect of copper loading of the SCR of NO by ethylene. Each sample had different copper loadings, depending on how many times it was subjected to ion exchange. There was no conversion when Ti-PILC (0 wt.% of Cu) was used as a catalyst for SCR of NO. Therefore Cu species must play a significant role in this catalytic reaction. Figure 3 shows the results of different Cu-Ti-PILC catalysts for SCR of NO by ethylene as a function of temperature. It can be observed that the introduction of copper into the catalyst causes enhancement of the catalytic activity. Increasing copper loading increased NO conversion until the copper loading reached 245% ion exchange. After this level, a further increase of copper loading led to a decrease of NO conversion. It was summarized in Table 3 that the increase of copper loading decreases the surface area and pore volume of the catalysts. The increase of Cu loading might result in an increase of CuO cluster formation. Therefore, although the sample had a higher Cu loading, some significant part of its active sites were not available for SCR of NO. It should also be noted from Fig. 3 that the increase in copper loading resulted in a shift of T_{max}, the temperatur maximum NO conversion, to lower values.

The activity for SCR of NO with Cu-ZSM-5 also depended on copper exchange level [6, 74]. However, the exchange level for the maximum NO conversion of Cu-Ti-PILC (245%) was different from that of Cu-ZSM-5 (80-100%).

3.5. The method of Cu introduction

The introduction of Cu onto Ti-PILC resulted in the enhancement of catalytic activity. In our experiment, the influence of the method of Cu addition on SCR activity was studied.

Figure 4 shows the SCR activities of two catalysts prepared by ion exchange (Cu-Ti-PILC) and incipient wetness impregnation (Cu/ Ti-PILC). The two samples had the same amount of Cu (5.9%). It was found that the Cu-ion-exchanged-Ti-PILC gave higher NO conversion than Cu-doped-Ti-PILC. This result could be due to two reasons: the nature of the Cu active sites, and the exposed Cu surfaces. The Cu species could be present either as isolated Cu ions or as CuO. The Cu species in Cu-Ti-PILC were mostly isolated Cu ions rather than CuO clusters. In contrast, the introduction of Cu by impregnation would form clusters of CuO. The surface area of the Cu- -Ti-PILC was 346 m^2/g, whereas that of Cu/Ti-PILC was 245 m^2/g. Although these two samples contained the same level of copper loading, the catalyst prepared by ion exchange had more available active sites for SCR of NO. Further work is needed to elucidate the nature of the Cu actives site for this reaction.

3.6. The promoting effect of Ce

Cerium (Ce) is known to be an active promoter for enhancing the activity for SCR of NO on PILC catalysts [57]. 0.5 and 1.0 %(wt) Ce_2O_3 were added to the Cu-Ti-PILC catalyst by impregnation. The SCR activities of 0.5% and 1.0% Ce-Cu-Ti-PILC for SCR of NO by C_2H_4 are shown in Fig. 5, and compared with the activity of Cu-Ti-PILC. The results in Fig. 5 a) show that 0.5% Ce-Cu-Ti-PILC increased NO conversion while 1.0% Ce-Cu-Ti-PILC decreased NO conversion. The BET surface areas were measured and it was found that 0.5% Ce_2O_3 caused a small decrease in BET surface area (from 346 to 333 m^2/g) whereas 1.0% Ce_2O_3 caused a large decrease in BET surface area (from 346 to 201 m^2/g). It can be concluded that 1.0% Ce-Cu-Ti-PILC contained large Ce_2O_3 clusters that could block the active surfaces for NO reduction leading to the decrease in NO conversion. However, Fig. 5 b) shows that both 0.5% and 1.0% Ce_2O_3 decreased the C_2H_4 conversion. Therefore Ce-Cu-Ti-

PILC catalysts are less active for hydrocarbon oxidation compare to Cu-Ti-PILC. It can be concluded that the addition of Ce results in the higher selectivity of catalyst for NO reduction.

3.7. Effect of H_2O and SO_2 on SCR of NO by Ethylene

Since all combustion gases contain water vapor and SO_2, the effects of H_2O and SO_2 are important. Although Cu-ZSM-5 has been the most extensively studied catalyst because of its high activity, the deactivation of Cu-ZSM-5 by the presence of H_2O and SO_2 is severe and has been discussed in a number of studies [66, 67]. In our experiments, the effects of H_2O and SO_2 on SCR of NO by ethylene on Cu-Ti-PILC, 0.5%Ce-Cu-Ti-PILC and Cu-ZSM-5 catalysts were measured and the results are shown in Fig. 6 and Fig. 7. The results show that H_2O and SO_2 decreased the activity of Cu-Ti-PILC and Ce-Cu-Ti-PILC only slightly as compared to Cu-ZSM-5. It was also found that the effect of H_2O was reversible following the removal of H_2O from the gas stream. On the other hand, the effect of SO_2 was reversible after a short term exposure (l hr) but it was not totally reversible after a long period of exposure (5hr). It was found from the product analysis that H_2O and SO_2 affected both NO and C_2H_4 conversion and they caused less inhibiting effect in the higher temperature range. Their inhibiting effects can be related to their adsorption on active sites both for NO reduction and C_2H_4 oxidation.

3.8. Reducing agent

One of the problems for the practical application of SCR of NO to real exhaust gases is related to reducing agents. Ammonia has be accepted as the reductant for SCR of NO in power plants. Ethylene and propylene have been used as typical reducing agents. Recently, methane has been tested as the reducing agent for SCR of NO with catalysts such as Co-ZSM-5 and Ga-ZSM-5.

In our experiments we studied SCR of NO by NH_3, C_2H_4 and CH_4 with Cu-Ti -PILC catalysts. The activity results are shown in Fig. 8. SCR of NO by NH_3 gave the highest NO conversion compared to SCR of NO by C_2H_4 or CH_4. NH_3 has higher selectivity for NO reduction partly because it contains nitrogen. Nitrogen is the result from coupling of two nitrogen atoms from NH_3 and NO. The result also show that Cu-Ti-PILC was inactive for SCR of NO by CH_4.

It is interesting to compare the NH_3 SCR results of Perathoner and Vaccari [65] with ours. Our space velocity was approximately twice as high as theirs (i.e., 60,000 vs. 30,000 h^{-1}), while other conditions were similar. The activities of the Cu-Ti-PILC were nearly as high as their Cu-Fe/Al-PILC, i.e., Cu^{2+} exchanged on a Fe_2O_3 and Al_2O_3 mixed pillared clay.

3.9. Ion-exchanged-Ti-PILC with other cations

Many ion-exchanged-ZSM-5 catalysts have been studied for their activities of SCR of NO. Cu-ZSM-5, Co-ZSM-5, Ce-ZSM-5, Pt-ZSM-5, Fe-ZSM-5, and Ga-ZSM-5, have all shown high activities. In our experiments, many ion-exchanged-Ti-PILC catalysts were also studied for SCR of NO by C_2H_4. It is important to note that there was no N_2O formation for SCR of NO by all ion-exchanged-Ti-PILC catalysts. This result was obtained by product analysis by using gas chromatography. The activities as a function of temperature for Cu-Ti-PILC, Fe-Ti-PILC, Co-Ti-PILC, Ce-Ti-PILC, Ag-Ti-PILC and Ga-Ti-PILC are compared in Fig. 9 as NO conversions.

The results in Fig. 9 show that Cu-Ti-PILC was the most active catalyst compared to other cation-exchanged forms. By comparing the NO conversion and C_2H_4 conversion, it is clear that the C_2H_4 oxidation was a catalyzed reaction, and was not a homogeneous reaction. The Cu-form was clearly the most active catalyst for C_2H_4 oxidation, whereas the Co-form

was the least active. For the Co-form, the conversions of NO and C_2H_4 were approximately equal at temperatures below 400°C, so the stoichiometry of the SCR reaction was 2NO/ C_2H_4. At temperatures higher than 400°C, C_2H_4 oxidation by O_2 became significant for the Co-form. An analysis of the NO conversion vs. C_2H_4 conversion from Fig. 9 indicates that the following two reaction stoichiometries were taking place:

$$2NO + C_2H_4 + 2O_2 \rightarrow N_2 + 2CO_2 + 2H_2O$$

$$nC_2H_4 + 3nO_2 \rightarrow 2nCO_2 + 2nH_2O$$

The ratio of the NO Conversion/C_2H_4 Conversion = 2/(1+n).

The value of n was associated with the C_2H_4 oxidation acitivity. Since the activation energy for C_2H_4 oxidation was higher than that for the SCR reaction, the value of n increased for any given catalyst with temperature. The behavior of Ga-Ti-PILC was unique in that its SCR activity was the highest in the high temperature range (> 450°C). This was similar to the ion-exchanged ZSM-5 by Ga^{3+}.

References

[1] H. Bosch and F. Janssen, Catal Today, 2 (1988) 369.

[2] M. Shelef, Chem. Rev., 95 (1995) 209.

[3] B.K. Cho, J. Catal., 142 (1993) 418.

[4] K.C. Taylor, in J.R. Anderson and M. Boudart (Editors), Catalysis: Science and Technology, Vol. 5, Springer-Verlag, Berlin, 1984.

[5] M. Iwamoto, Symposium on Catalytic Technology for Removal of Nitrogen Oxides, Catal. Soc. Japan, 1990, p. 17-22.

[6] M. Iwamoto and N. Mizuno, J. Auto. Eng., 207 (1993) 23.

[7] W. Held, A. König, T. Richter and L. Puppe, SAE Paper 900469, (1990).

[8] M. Iwamoto and H. Yahiro, Catal. Today, 22 (1994) 5.

[9] J. Valyon and W.K. Hall, J. Catal., 143 (1993) 520.

[10] J. Petunchi, G.A. Sill and W.K. Hall, Appl. Catal. B, 2 (1993) 303.

[11] A.P. Ansell, A.F. Diwell, S.E. Columski, J.W. Hayes, R.R. Rajaran, T.J. Truex and A.P. Walker, Appl. Catal. B, 2 (1993) 101.

[12] C.H. Bartholomew, R. Gopalakrishnan, P.R. Stafford, J.E. Davison and W.C. Hecker, Appl. Catal., B, 2 (1993) 183.

[13] Y. Li and J.N. Armor, Appl. Catal. B, 3 (1994) L1.

[14] D.J. Liu and H.J. Robota, Appl. Catal. B, 4 (1994) 155.

[15] Z. Chajar, M. Primet, H. Praliaud, M. Chevrier, C. Gauthier and F. Mathis, Appl. Catal. B, 4 (1994) 199.

[16] J. Dedecek, Z. Sobalik, Z. Tvaruzkova, D. Kaucky and B. Wichterlova, J. Phys. Chem. 99 (1995) 16327.

[17] K.C.C. Kharas, D.J. Liu and H.J. Robota, Catal. Today, 26 (1995) 129.

[18] B.J. Adelman, T. Beutel, G.D. Lei and W.M. H. Sachtler, J. Catal., 158 (1996) 327.

[19] V.A. Matyshak, A.N. Ilichev, A.A. Ukharsky and V.N. Korchak, J. Catal., 171 (1997) 245.

[20] C. Torre-Abreu, M.F. Ribeiro, C. Henriques and F.R. Ribeiro, Appl. Catal., B, 11 (1997) 383.

[21] Y. Li and J. N. Armor, Appl. Catal., B, 1 (1992) L31.

[22] F. Witzel, G.A. Sill and W.K. Hall, J. Catal., 149 (1994) 229.

[23] Y. Li and J. N. Armor, J. Catal., 150 (1994) 376.

[24] Y. Li, T.L. Slager and J. N. Armor, J. Catal., 150 (1994) 388.

[25] Y. Zhang, A. Patwardhan, Z. Li, A. Sarofim and M. Flytzani-Stephanopoulos, paper persented at AIChE Annual Meeting, Paper 82f, Miami, FL., Nov. 15, 1995.

[26] Y. Li and J. N. Armor, Appl. Catal, B5, (1995) L 257.

[27] M.C. Campa, S.D. Rossi, G. Ferrsris and V. Indovina, Appl. Catal. B, 8 (1996) 315.

[28] A. Yu. Stakheev, C.W. Lee, S.J. Park and P.J. Chong, Appl. Catal., B, 9 (1996) 65.

[29] T. Liese and W. Grunert, J. Catal., 172 (1997) 34.

[30] M. Misono and K. Konodo, Chem. Lett., (1991) 1001.

[31] C. Yokoyama and M. Misono, J. Catal., 150 (1994) 9.

[32] S. Sato, H. Hirabayashi, H. Yahiro, N. MiZuno and M. Iwamoto, Catal. Lett., 12 (1992) 193.

[33] X. Feng and W.K. Hall, J. Catal., 166 (1997) 368.

[34] W.M.H. Sachtler and H.Y. Chen, Chem. & Eng. News, September 15 (1997) 8.

[35] C. Rottlander, R. Andorf, C. Plog, B. Krutsch and M. Baerns, Appl. Catal., **B11** (1996) 49.

[36] H. Kato, C. Yokoyama and M. Misono, Catal. Lett. 47 (1997) 189.

[37] A.W. Aylor, L.J. Lobree, J.A. Reimer and A.T. Bell, J. Catal., 170 (1997) 390.

[38] K. Yogo, S. Tanaka, M. Ihara, T. Hishiki and E. Kikuchi, Chem. Lett., (1992) 1025.

[39] Y. Li and J.N. Armor, J. Catal., 145 (1994) 1.

[40] K.A. Bethke, D. Alt and M.C. Kung, Catal. Lett., 25 (1994) 37.

[41] M. Kung, K. Bethke, D. Alt, B. Yang and H. Kung in U.S. Ozkan, S. Agarwal and C. Marcelin (Editors), No_x Reduction, Chap. XX, ACS Symp., Ser., ACS, Washington, DC, 1995.

[42] K.A. Bethke and H.H. Kung, J. Catal., 172 (1997) 93.

[43] T.E. Hoost, R.J. Kudla, K.M. Collins and M.S. Chattha, Appl. Catal., B13 (1997) 59.

[44] R. Burch and T.C. Watling, Appl. Catal., B11 (1997) 207.

[45] M.W. Kumthekar and U.S. Ozkan, J. Catal., 171 (1997) 54.

[46] U.S. Ozkan, M.W. Kumthekar and G. Karakas, J. Catal., 171 (1997) 67.

[47] M. Ozawa, H. Toda and S. Suzuki, Appl. Catal., B8 (1996) 141.

[48] F.H. Dekker, S. Kraneveld, A. Bliek, F. Kapteijn and J. A. Moulijn, J. Catal., 170 (1997) 168.

[49] J.Y. Yan, M.C. Kung, M.W.H. Sachtler and H.H. Kung, J. Catal., 172 (1997) 178.

[50] A. Ueda, T. Ohima and M. Haruta, Appl. Catal. B12 (1997) 81.

[51] M.A. Vannice, A.B. Walters and X. Zhang, J. Catal., 159 (1996) 119.

[52] J.S. Feeley, M. Deeba, R.J. Farrauto, G. Beri and A. Haynes, Appl. Catal. B6, (1995) 79.

[53] M.D. Amiridis, T. Zhang and R.J. Farrauto, Appl. Catal., B10 (1996) 203.

[54] A. Fritz and V. Pitchon, Appl. Catal., 13 (1997) 1.

[55] W.C. Wong and K. Nobe, Ind. Eng. Chem. Prod. Res. Dev. 25 (1986) 179.

[56] R.T. Yang, T.J. Pinnavaia, W.B. Li and W. Zhang, J. Catal. 172 (1997) 488.

[57] R.T. Yang and W.B. Li, J. Catal., 155 (1995) 414.

[58] W.B. Li, M. Sirilumpen and R.T. Yang, Appl. Catal., 11 (1997) 347.

[59] R.T. Yang and L.S. Cheng, "Pillared Clays and Ion Exchanged Pillared Clays as Gas Adsorbents and as Catalysts for Selective Catalytic Reduction of NO," in Access in Nanoporous Materials, T.J. Pinnavaia and M. Thorpe (Editors), pp 73-93, Plenum, New York (1995).

[60] R.T. Yang and J.E. Cichanowicz, Pillared Interalered Catalysts for the Selective Catalytic Reduction of Nitric Oxide with Ammonia, U.S. Patent 5,415,850 (1995).

[61] R.T. Yang, J.P. Chen, E.S. Kikkinides, L.S. Cheng and J.E. Cichanowicz, Ind. Eng. Chem. Res., 31 (1992) 144.

[62] J.P. Chen, M.C. Hausladen and R.T. Yang, J. Catal., 151 (1995) 135.

[63] L.S. Cheng, R.T. Yang and N. Chen, J.Catal., 164 (1996) 70.

[64] M. Sirilumpen, R.T. Yang and N. Tharapiwattananon, J. Molecular Catal., A (1998), in press.

[65] S. Perathoner and A. Vaccari, Clay Minerals, 32 (1997) 123.

[66] Y. Li and J.N. Armore, Appl. Catal., B5 (1995) L 257.

[67] M. Iwamoto, N. Mizuno and H. Yahiro, Proc. 10th Intern. Cong. Catal., Hungary (1992) 1285.

[68} M.P. Atkins, in I.V. Mitchell (Editor), Pillared Layeres Structures, Current Trends and Applications, Elsevier, New York, (1990) 159.

[69] K. Bahranowski, R. Dula, R. Grabowski, B. Grzybowska-Swierkosz, E.M. Serwicka and K. Wcislo, Book of Abstract Europacat II, Maastricht, (1995) 210.

[70] C.F. Baes, R.E. Mesmer, The Hydrolysis of Cations, Wiley, New York, 1976.

[71] R. Burch, Catal. Today, 2 (1988) 185.

[72] J. Sterte, Clays & Clay Miner., 34 (1986) 658.

[73] S. Yamanaka and W. Brindley, Clays & Clay Miner., 27 (1979) 119.

[74] G.M. Brindley and R.E. Sempels, Clays & Clay Miner., 25 (1977) 229.

[75] R.A. Schoonheydt, H. Leeman, A. Scorpion, I. Lenotte and P. Grobet, Clays & Clay Miner., 42 (1994) 518.

[76] S. Sato, Y. Yu, H. Yahiro, N. Mizuno and M. Iwamoto, appl. Catal., 70 (1991) L1.

Table 1. Physical Characterization: BET Surface Area, Pore Volume, Inter-layer Spacing

PILC	BET surface area (m^2/g)	Pore volume cm3/g	d(001) Å	Spacing Å
Fisher bentonite	34	0.07	9.87	
$A1_2O_3$-PILC	209	0.15	17.83	8.23
ZrO_2-PILC	195	0.14	18.98	9.38
TiO_2-PILC*	383	0.29		
$A1_2O_3$-PILC	384	0.30	19.50	9.90
$A1_2O_3$-Laponite*	467	0.39		

* Delaminated forms.

Table 2. Copper Content (in wt%) of Cu^{2+} -ion exchanged-PILC

PILC	% Cu	% ion exchange
Cu-Ti-PILC	5.928	245.49[a]
Cu-Zr-PILC	2.924	121.09
Cu-Al-PILC	3.842	159.10
Cu-Al-Lapo	4.157	139.19
Cu-ZSM-5	3.44	238.26[b]

a: Degree of ion exchange of PILC = (2*number of CU)* 100/CEC

b: Degree of ion exchange of Cu^{2+}ZSM-5 = (2*number ofCu)*1OO/number of Al

Table 3. BET Surface Area and Pore Volume of Cu-Ti- PILCs

% Ion exchange	BET surface area (m^2/g)	Pore volume (cm^3/g)
0	383.08	0.29
43	372.26	0.28
100	358.35	0.28
245	345.84	0.27
313	277.17	0.23

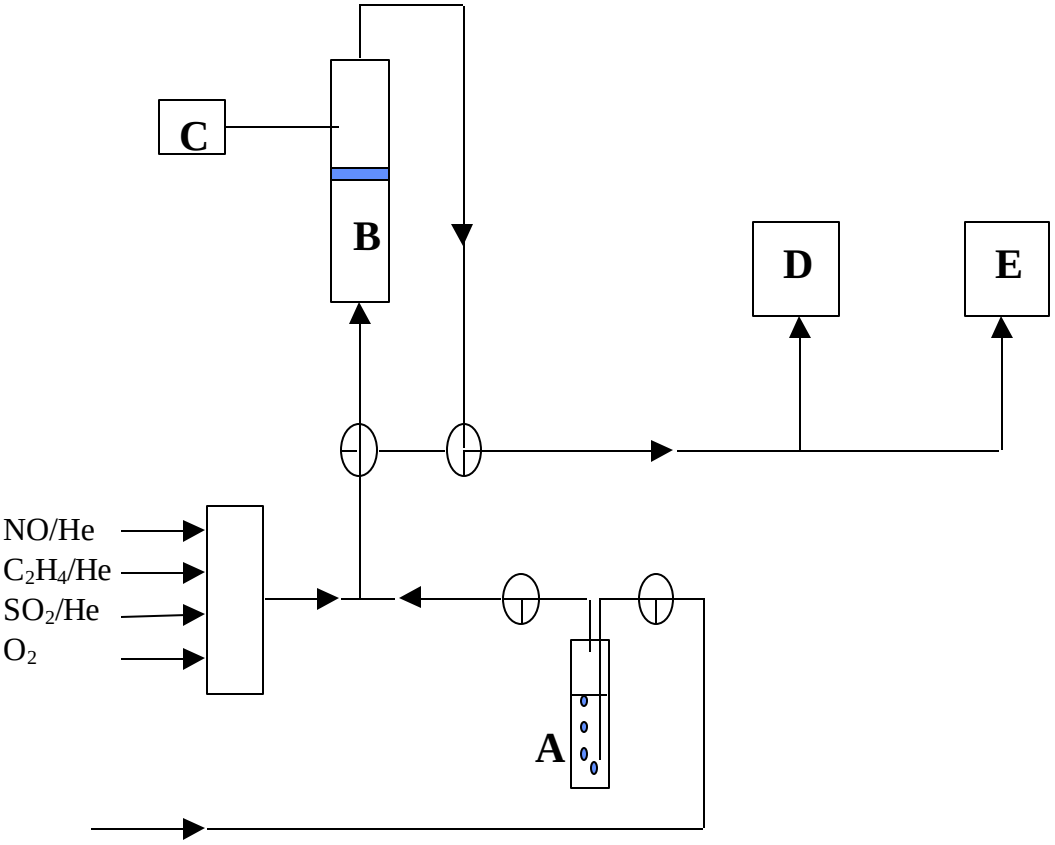

Fig. 1. The scheme of apparatus for the SCR reaction.

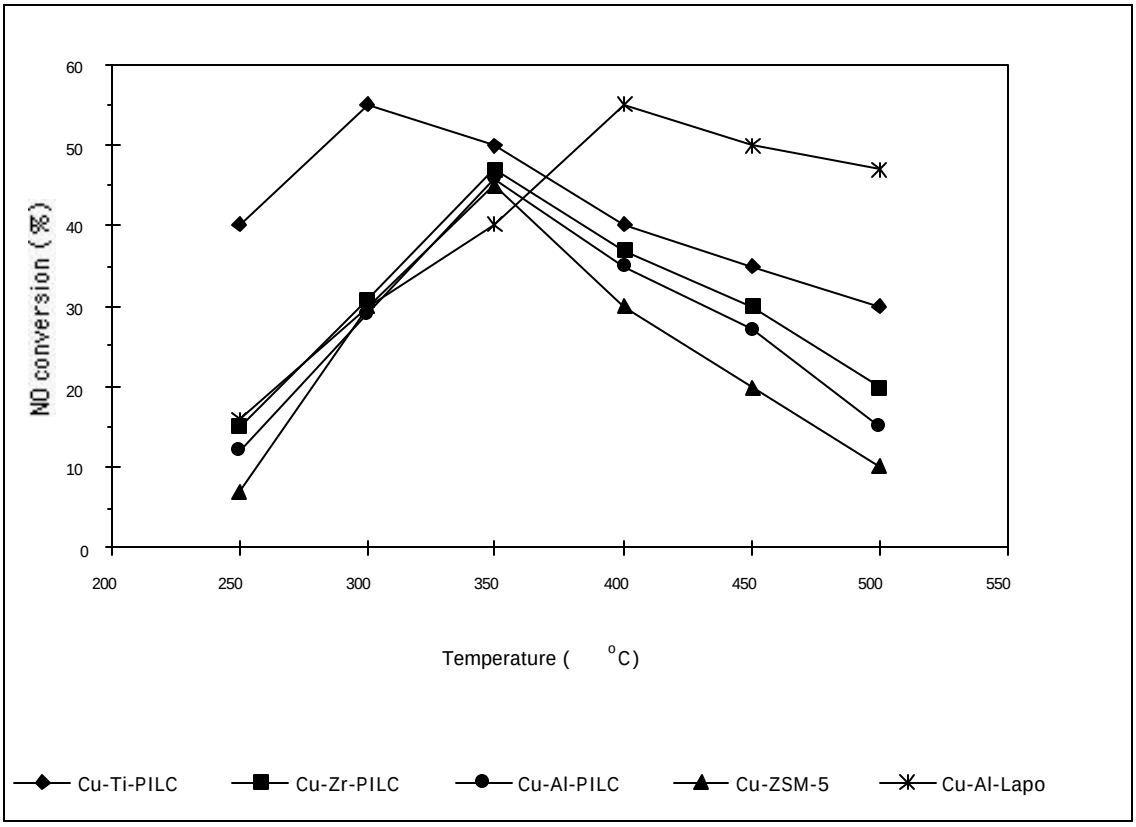

Fig. 2. SCR activities over Cu-Ti-PILC, Cu-Zr-PILC, Cu-Al-PILC, Cu-Al-Laponite and Cu-ZSM-5 for NO reduction by ethylene. Reaction conditions: NO = C_2H_4 = 1000 ppm, O_2=2%, catalyst = 0.5g, He = balance and total flow rate =250 cc/min.

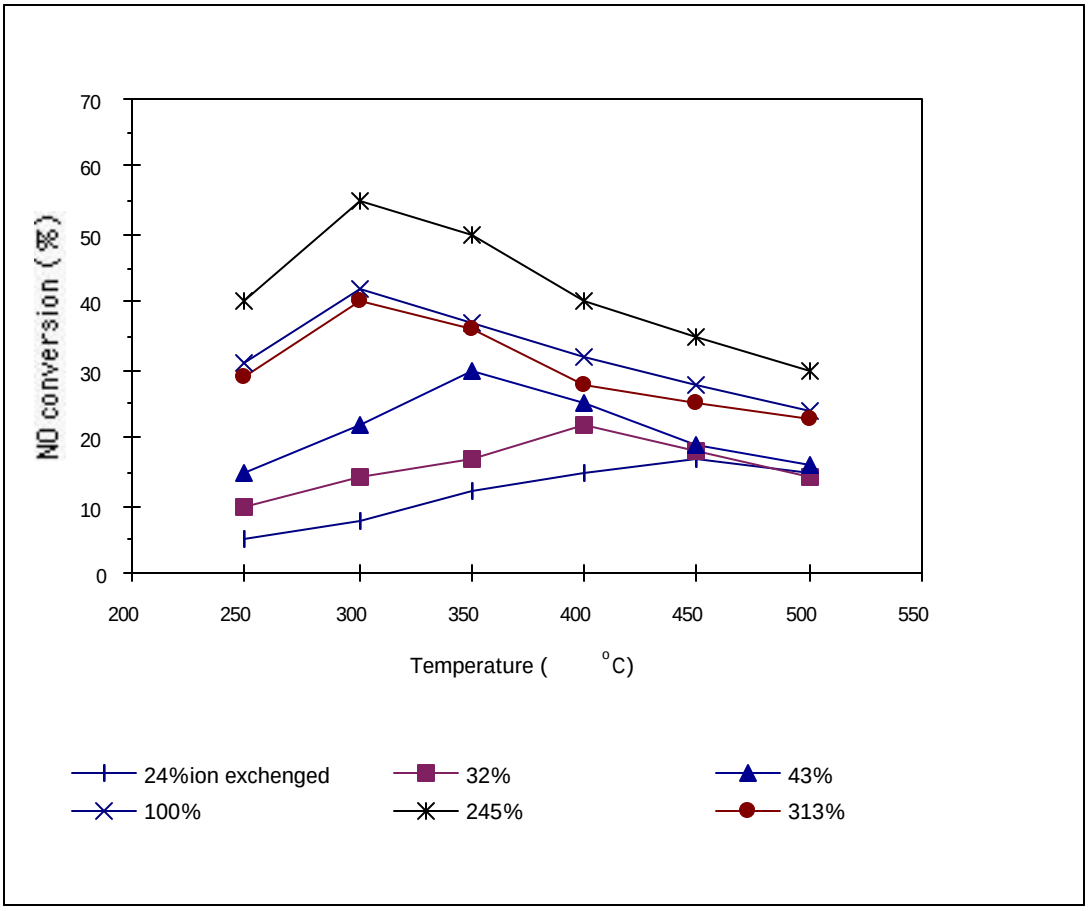

Fig. 3. Effect of copper loading of Cu-Ti-PILC on NO conversion for SCR of NO by ethylene. Reaction conditions: NO = C_2H_4 = 1000 ppm, O_2 = 2%, catalyst = 0.5g, He = balance and total flow rate =250 cc/min.

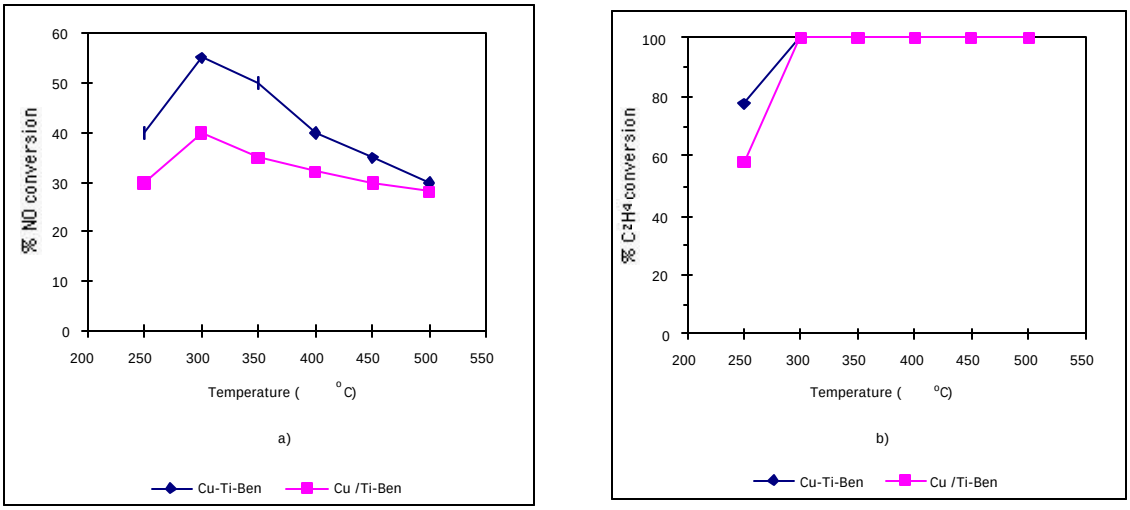

Fig. 4. SCR activities over Cu-exchanged-Ti-PILC (Cu-Ti-PILC) and Cu-doped-Ti-PILC (Cu/Ti-PILC), both with 5.9% (wt.) Cu. a) % NO conversion and b) % C_2H_4 conversion. Reaction condition: NO = C_2H_4 = 1000 ppm, 0_2 = 2%, catalyst = 0.Sg, He = balance and total flow rate = 250 cc/min.

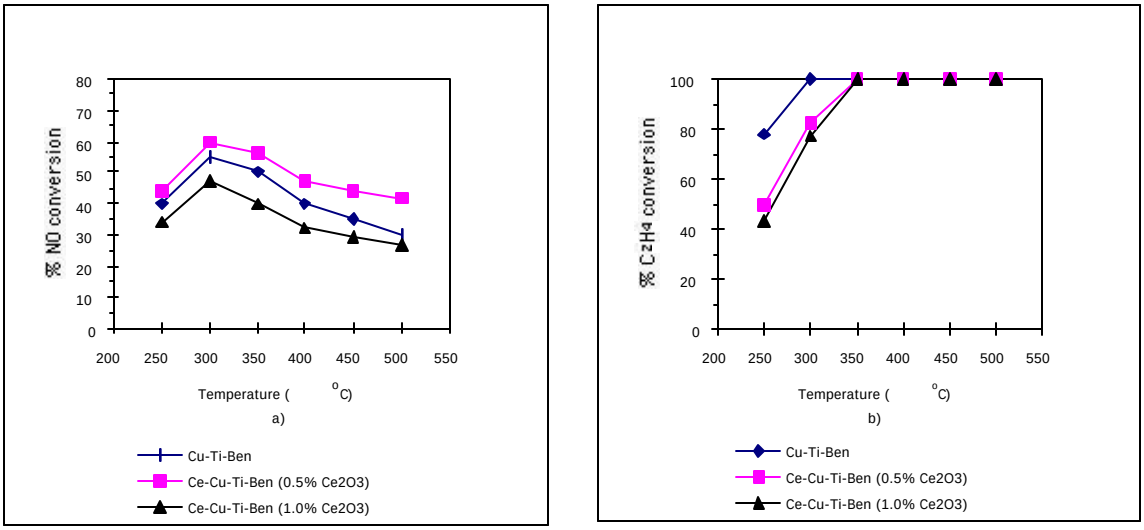

Fig. 5. Promoting effect of Ce_2O_3 on SCR of NO by ethylene with Cu-Ti-PILC: a) % NO conversion and b) % C_2H_4 conversion. Reaction conditions: NO = C_2H_4 = 1000 ppm, O_2 = 2%, catalyst = 0.Sg, He = balance and total flow rate = 250 cc/min.

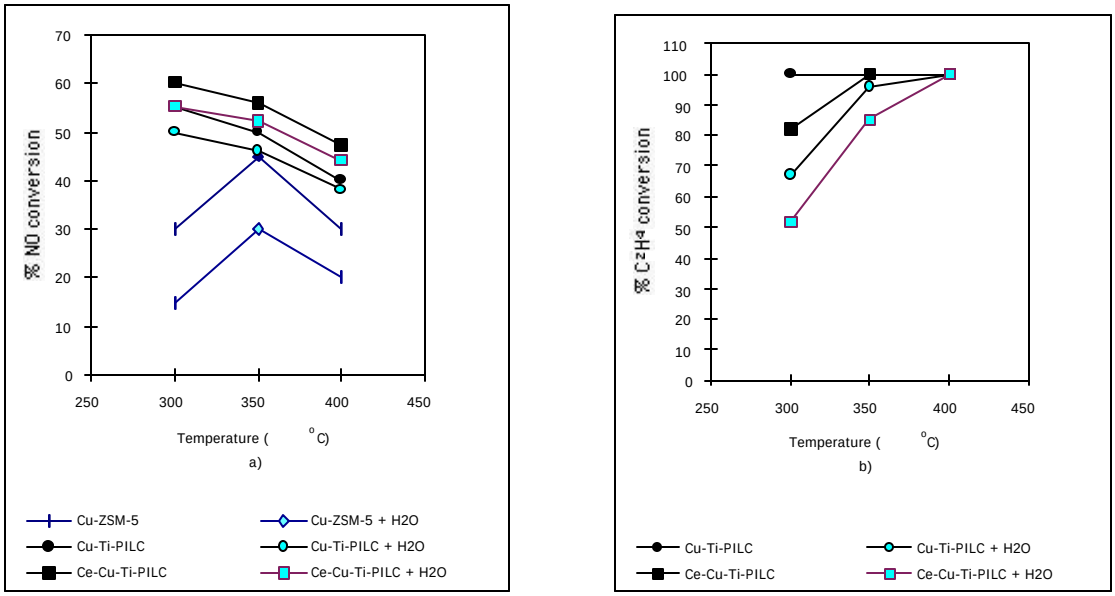

Fig. 6. H_20 effect on SCR of NO by ethylene with Cu-Ti-PILC: a) % NO conversion and b) % C_2H_4 conversion. Reaction conditions: NO = C_2H_4 = 1000 ppm, O_2 = 2%, H_2O = 5 %, catalyst = 0.Sg, He = balance and total flow rate = 250 cc/min.

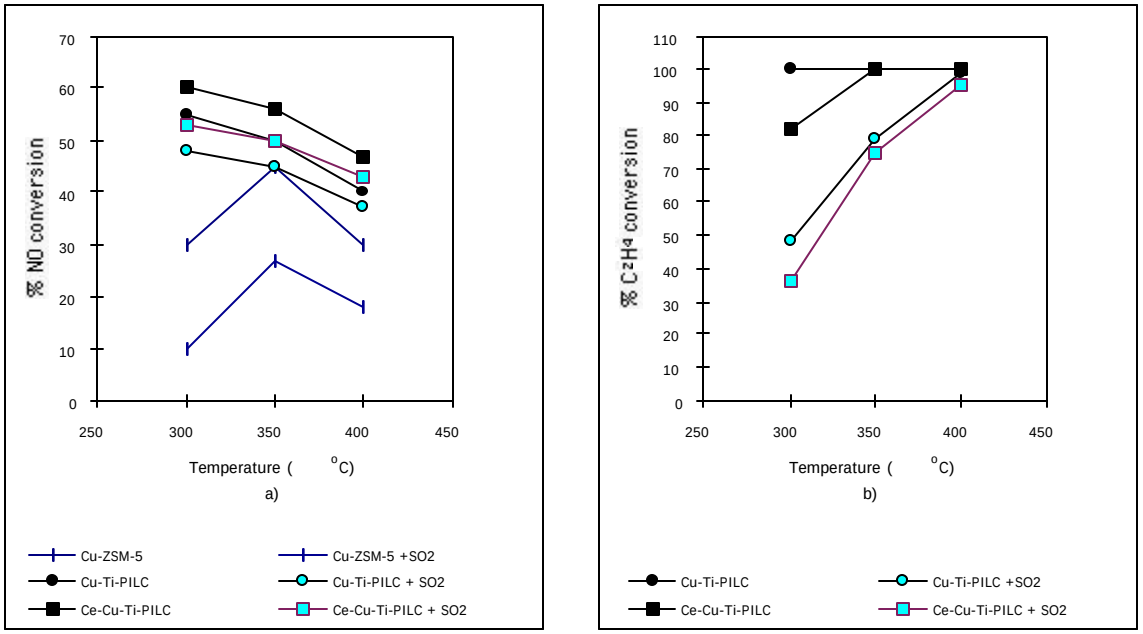

Fig. 7. SO_2 effect on SCR of NO by ethylene with Cu-Ti-PILC: a) % NO conversion and b) % C_2H_4 conversion. Reaction conditions: NO = C_2H_4 = 1000 ppm, O_2 = 2%, SO_2 = 500 ppm, catalyst = 0.Sg, He = balance and total flow rate = 250 cc/min.

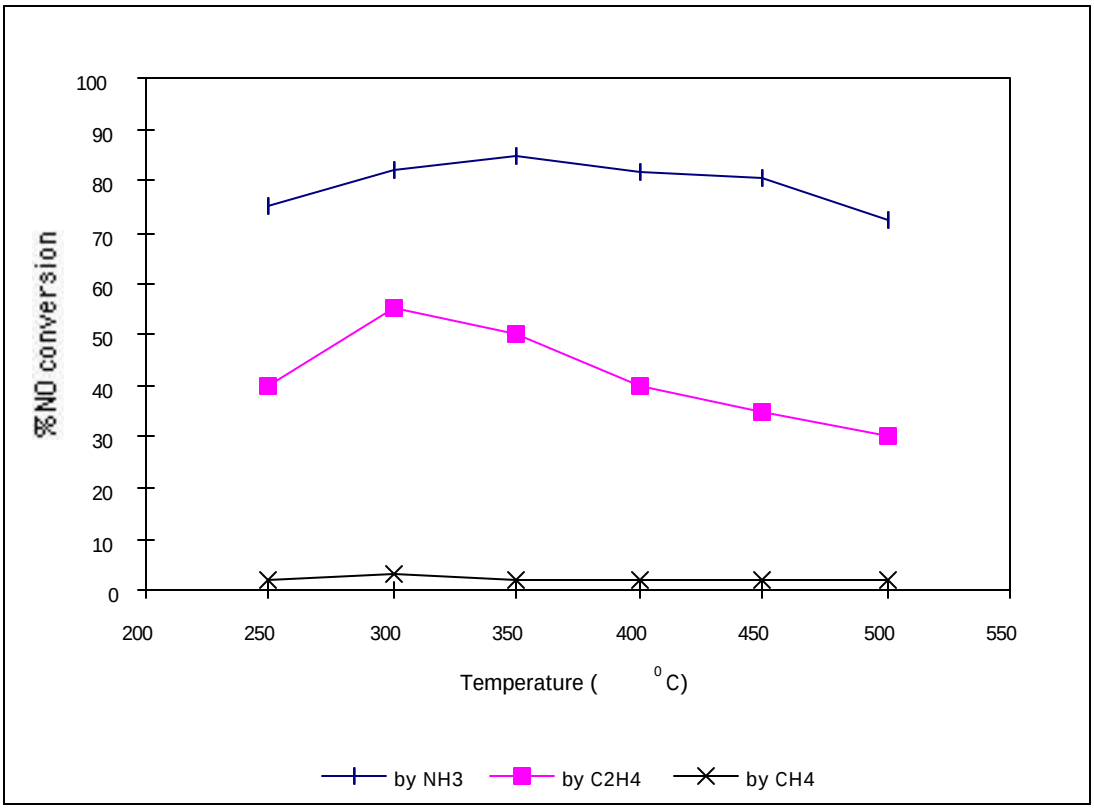

Fig. 8. SCR activities over Cu-Ti-PILC by ethylene, methane and ammonia. Reaction conditions: NO = 1000 ppm, C_2H_4 = NH_3 = 1000 ppm (when used), CH_4 = 2000 ppm (when used), O_2=2%, catalyst = 0.5g, He = balance and total flow rate = 250 cc/min.

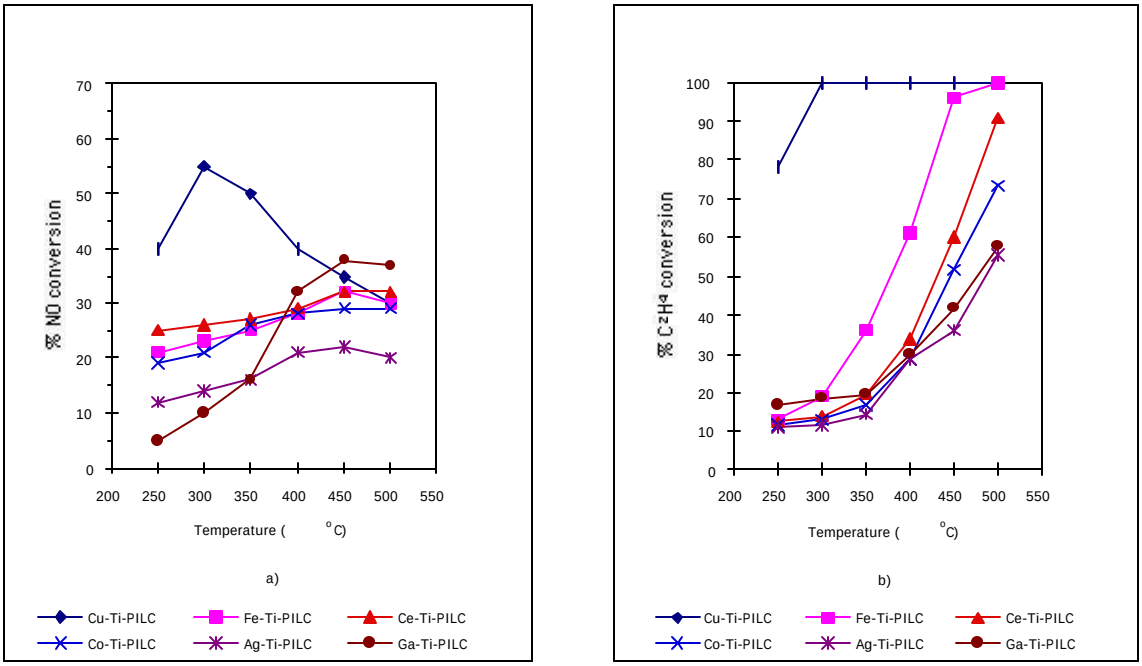

Fig. 9. SCR of NO by ethylene with Cu-Ti-PILC, Fe-Ti-PILC, Ce-Ti-PILC, Co-Ti-PILC, Ag-Ti-PILC, Ga-Ti-PILC: a) % NO conversion and b) % C_2H_4 conversion. Reaction conditions: NO = C_2H_4 = 1000 ppm, O_2=2%, catalyst = 0.5g, He = balance and total flow rate =250 cc/min.

CHAPTER TWO

Selective catalytic reduction of nitric oxides with ethylene on copper ion-exchanged Al-MCM-41 catalyst

1. Introduction

The selective catalytic reduction (SCR) of NO_x ($NO+NO_2$) with hydrocarbons is an attractive route for NO_x conversion to N_2 from exhaust gas. The three-way catalyst (Pt, Pd, and Rh) has been used commercially in gasoline engines for reduction NO to N_2 by carbon monoxide and hydrocarbons under rich-burn (O_2-lean) conditions, but it becomes ineffective in the presence of excess oxygen [1]. Since the reports by Iwamoto et al. [2] and by Held et al. [3] that copper ion-exchanged ZSM-5 could selectively reduce NO_x by hydrocarbons (e.g., C_2H_4, C_3H_6, C_3H_8, etc.) in the presence of excess oxygen, this topic has been extensively studied all over the word in recent years. Three comprehensive reviews on the reaction were recently presented by Shelef [4], Amiridis et al. [5], Fritz and Pitchon [6], respectively. Many catalysts, such as Cu-ZSM-5 [2, 3], Co-ZSM-5 and Co-Ferrierite [7-9], Cu^{2+}-exchanged pillared clay [10, 11], Pt/Al_2O_3 [12,13], Fe-ZSM5 [14, 15] and so on, have been found to be active in this reaction. Copper ion-exchanged zeolites (including ZSM-5, ferrierite, mordenite, Y zeolite, L zeolite, Beta zeolite, etc.) were also studied and compared directly under the same conditions [2, 16]. It was found that Cu-ZSM-5 showed the highest NO_x conversion but Cu-Y zeolite showed the lowest activity among the catalysts under the same conditions. It seems that the zeolite framework composition plays an important role for the copper ion-exchanged zeolites in the SCR reaction. Considering that MCM-41, which is a new member of the zeolite family with pore dimensions between 1.5 and 10 nm [17, 18], has a more open porosity than ZSM-5 and thus can enhance the diffusion of reactant under the reaction conditions, we have tried using ion-exchanged or doped MCM-41 as SCR (by NH_3 and hydrocarbons) catalyst recently [19, 20]. Because MCM-41 has high thermal stability, large BET surface area and

pore volume, it has been studied for potential use as catalysts, supports or sorbents during the last 5 years [21]. We found that platinum doped MCM-41 catalysts showed a higher specific activity than Pt/Al_2O_3 catalyst [20]. In this work, we will present first results on the activity of copper ion-exchanged Al-MCM-41 catalysts for selective catalytic reduction of NO_x by ethylene, using cerium as promoter.

2. Experimental

2.1 Preparation of catalyst

Fumed silica (99.8%, Aldrich), tetramethylammonium hydroxide pentahydrate (TMAOH, 97%, Aldrich),), 25 wt.% cetyltrimethylammonium chloride (CTMACl) in water (Aldrich), $Al[C_2H_5CH(CH_3)O]_3$ (97%, Aldrich) and NaOH (98.1%, Fisher) were used as source materials for preparing Al-MCM-41.

The Al-MCM-41 (Si/Al=10) sample was synthesized according to the procedure given by Borade and Clearfield [22]. Solution A was prepared by dissolving 1.325 g TMAOH in 100 ml deionized water and then adding 5 g fumed silica. Solution B was obtained by dissolving 0.72 g NaOH in deionized water and adding 25 ml CTMACl followed by adding 2.19 ml $Al[C_2H_5CH(CH_3)O]_3$ at room temperature. The two solutions were stirred for 10-15 min, then solution A was added to solution B. The reaction mixture had the following chemical composition $1SiO_2$-$0.05Al_2O_3$-0.23CTMACl-$0.11Na_2O$-0.089TMAOH-$125H_2O$. After being stirred for 15 min, the mixture was transferred into a 250 ml three-neck flask and was

then heated at 100 °C for 48 h. After filtering, the solid was washed, dried and calcined at 560 °C for 10 h in a flow of air (150 ml/min).

The copper and cerium ion-exchanged Al-MCM-41 were prepared by using conventional ion exchange procedure at room temperature. Solutions of 0.02 M $Cu(NO_3)_2$ (adjusting pH value to 4.5 by 2N HNO_3) and 0.02 M $Ce(NO_3)_3$ were used for exchange. The Ce-Cu-Al-MCM-41 catalyst was obtained from Cu^{2+} exchange of the Ce-Al-MCM-41 sample; Ce exchange was done first because it was harder than copper exchange. All the exchange processes were repeated three times and each time was carried out for 24 h. After the ion-exchange procedure, all the samples were calcined at 550 ^oC in air for 4 h. The Cu/Al in the Cu-Al-MCM-41 obtained by neutron activation analysis was 0.372 (i.e., 74.4% ion exchange), and Ce/Al in Ce-Al-MCM-41 was 0.164 (i.e., 49.2% ion exchange). In Ce-Cu-Al-MCM-41 sample, Ce/Al and Cu/Al were 0.053 and 0.37, respectively, i.e., 89.9% total ion exchange.

2.2 Characterization of catalyst

The powder X-ray diffraction (XRD) measurement was carried out with a Rigaku Rotaflex D/Max-C system with Cu K_α (λ = 0.1543 nm) radiation. The samples were loaded on a sample holder with a depth of 1 mm.

A Micromeritics ASAP 2010 micropore size analyzer was used to measure the N_2 adsorption isotherm of the samples at liquid N_2 temperature (-196 °C). The specific surface areas of the samples were determined from the linear part of the BET plots (P/P_0 = 0.05-0.20). The pore size distribution was also calculated from the desorption branch of the N_2 adsorption

isotherm using the Barrett-Joyner-Halenda (BJH) Formula, as suggested by Tanev and Vlaev [23], because the desorption branch can provide more information about the degree of blocking than the adsorption branch and the best results were obtained from the BJH formula. Prior to the surface area and pore volume measurements, samples were dehydrated at 350 °C for 4 h.

The reducibility of catalyst was characterized by temperature-programmed reduction (TPR) analysis. In each experiment, 0.1 g sample was loaded into a quartz reactor and then pretreated in a flow of He (40 ml/min) at 400 ^{o}C for 0.5 h. After the sample was cooled down to room temperature in He, the reduction of the sample was carried out from 30 to 700 ^{o}C in a flow of 5.34 % H_2/N_2 (27 ml/min) at 10 ^{o}C/min. The consumption of H_2 was monitored continuously by a thermal conductivity detector. The water produced during the reduction was trapped in a 5A molecular sieve column.

2.3 Catalytic performance evaluation of catalyst

The SCR activity measurement was carried out in a fixed-bed quartz reactor. The reaction temperature was controlled by an Omega (CN-2010) programmable temperature controller. 0.5 g sample, as particles of 60-100 mesh, was used in this work. The typical reactant gas composition was as follows: 1000 ppm NO, 1000 ppm C_2H_4, 0-7.5% O_2, 500 ppm SO_2 (when used), 5% water vapor (when used), and balance He. The total flow rate was 250 ml/min (ambient conditions). The premixed gases (1.01% NO in He, 1.04% C_2H_4 in He, and 0.99% SO_2 in He) were supplied by Matheson Company. The NO_x concentration was continuously monitored by a chemiluminescent NO/NO_x analyzer (Thermo Electro Corporation, Model 10). The other effluent gases were analyzed by a gas chromatograph (Shimadzu, 14A) at

50 °C with 5A molecular sieve column for O_2 , N_2 and CO, and Porapak Q column for CO_2, N_2O and C_2H_4.

3. Results

3.1 Characterization of catalyst

The powder XRD patterns of Al-MCM-41 and ion-exchanged Al-MCM-41 samples are measured. The pattern of Al-MCM-41 is consistent with that reported previously for the Al-MCM-41 molecular sieve [17, 18, 22] and all XRD peaks can be indexed on a hexagonal lattice with d_{100} = 4.1 nm. According to the value of d_{100}, the unit cell dimension (a=4.7 nm) was calculated by the formula a= $2d_{100}/\sqrt{3}$. After the sample was exchanged with copper ions and/or cerium ions, the shapes of XRD patterns were essentially unchanged, indicating that the ion exchange process did not affect the framework structure of this molecular sieve. No oxide phase (CuO or Ce_2O_3) was detected in these samples.

The BET specific surface area, pore volume, average pore diameter of the Al-MCM-41 and ion-exchanged Al-MCM-41 samples are summarized in Table 1. These samples were found to have narrow pore size distributions with pore size of ca. 4.2 nm, high BET specific surface areas (ca. 900 m^2/g) and high pore volumes (> 1.00 cm^3/g).

TPR can be used to identify and quantify the copper species in copper ion-exchanged zeolite [24]. No H_2 consumption was found on the Ce^{3+}-exchanged Al-MCM-41 sample below 700 ^oC, indicating that the Ce^{3+} in the framework of Al-MCM-41 is very hard to be reduced to lower valence. For Cu-Al-MCM-41 and Ce-Cu-Al-MCM-41 samples, the TPR

profiles showed two reduction peaks, which suggests a two-step reduction process of isolated Cu^{2+} species [24]. One peak appeared at a lower temperature, indicating that the process of $Cu^{2+} \rightarrow Cu^{+}$ occurred. The other peak at a higher temperature suggests that the produced Cu^{+} was further reduced to Cu^{0}. According to these results, we can conclude that no CuO aggregates existed in the two copper ion-underexchanged Al-MCM-41 samples (i.e., Cu/Al < 0.5) because the CuO aggregates would be reduced to Cu^{o} by H_2 in one step at about 230 ^{o}C if they existed in the two samples [24]. This was in line with the above XRD result that no CuO phase was detected in the two samples. Copper in the Cu-Al-MCM-41 and Ce-Cu-Al-MCM-41 mainly existed in the form of isolated copper ions. Delahay et al. also reported that copper was mainly present as isolated Cu^{2+} species in underexchanged Cu-Beta and Cu-MFI zeolites [24]. The ratios of H_2 consumption to Cu for the second peak ($Cu^{+} \rightarrow Cu^{0}$) in the two samples were close to 0.5 (Table 1); by comparison, the H_2/Cu ratios for the first peak ($Cu^{2+} \rightarrow Cu^{+}$) were lower than 0.5 (Table 1). This phenomenon could be accounted for as the result of partial reduction of Cu^{2+} to Cu^{+} during the course of catalyst preparation (calcination at 550 ^{o}C) or pretreatment at 400 ^{o}C in a flow of He. In addition, the reduction temperatures of Ce-Cu-Al-MCM-41 were about 20 ^{o}C lower than those of Cu-Al-MCM-41 (323 ^{o}C vs. 342 ^{o}C and 540 ^{o}C vs. 561 ^{o}C), suggesting that the Cu^{2+} and Cu^{+} ions in the former are more easily reduced than those in the latter. This is reasonable because when Na^{+} in the Al-MCM-41 was partially substituted by Ce^{3+}, the positive charges in the framework would increase and thus lead to weaker electrostatic interactions between Al-MCM-41 and the copper ions. As expected, this would also result in a lower Cu^{2+}/Cu^{+} ratio in the Ce-Cu-Al-MCM-41 than that in the Cu-Al-MCM-41 (0.73 vs. 0.80, as shown in Table 1) after the samples were treated at 400 ^{o}C in He.

3.2 NO_x reduction activity of catalyst

The catalytic performance of the catalysts for SCR reaction of NO_x with C_2H_4 as functions of the reaction temperature are summarized in Fig. 1 and Fig. 2. Ce^{3+}-exchanged Al-MCM-41 was found to be inactive in this reaction at 250-600 °C; almost no NO_x was reduced to N_2, but some C_2H_4 was oxidized to CO_2 by O_2 at higher temperatures. Over the Cu-Al-MCM-41 and Ce-Cu-Al-MCM-41 catalysts, only a small amount of NO_x was converted to N_2 at 250 ^oC. With the increase of reaction temperature, NO_x conversion increased, passing through a maximum, then decreased at higher temperatures. No nitrous monoxide and carbon monoxide were detected in the temperature range and N_2 was the only product containing nitrogen. The nitrogen balance and carbon balance were both above 95% in this work. The decrease in NO_x conversion at higher temperatures was due to the combustion of ethylene. Ce-Cu-Al-MCM-41 always showed higher NO_x conversions than Cu-Al-MCM-41, indicating that cerium ions played an important promoting effect in the catalyst (because no activity was obtained on Ce-Al-MCM-41 sample). The maximum NO_x conversion reached 38% at 550 ^oC over the Ce-Cu-Al-MCM-41 catalyst, which was about 15% higher than that over Cu-Al-MCM-41. The ethylene conversion reached 100% at 500 °C on Cu-Al-MCM-41 catalyst. The conversions of ethylene on Ce-Cu-Al-MCM-41 were found to be lower than those on Cu-Al-MCM-41 (Fig. 2).

It is well known that oxygen is important in the SCR reaction of nitric oxides by hydrocarbons [2-6]. The effect of O_2 concentration on NO_x conversion to N_2 was also investigated at 500 °C on Ce-Al-Cu-MCM-41 catalyst. As shown in Fig. 3, almost no NO_x

reacted with ethylene in the absence of O_2. After O_2 was introduced into the feed mixture, NO_x conversion was significantly increased. This indicates that oxygen plays an important role for the reduction of NO_x by C_2H_4, as we expected. The maximum conversion reached ca. 38% in the presence of 1-1.6% O_2 . After that, NO_x conversion was found to decrease slightly at higher O_2 concentrations. C_2H_4 conversion always increased with the increase of O_2 concentration.

4. Discussion

When sodium ions in Al-MCM-41 were partially exchanged by copper ions or copper and cerium ions, the Cu-Al-MCM-41 and Ce-Cu-Al-MCM-41 catalysts showed a high activity in SCR reaction of NO_x by ethylene in the presence of excess oxygen. Since the samples without copper (i.e., Al-MCM-41 and Ce-Al-MCM-41) showed little or no activity in this reaction, copper ions clearly play an important role for the reduction of NO_x to N_2. Iwamoto and co-workers studied the effect of zeolite structure on the catalytic performance of SCR reaction by comparing NO_x conversion on different zeolites exchanged with copper ions [2, 16]. In addition to Cu-ZSM-5 (Si/Al = 11.7), Cu^{2+}-exchanged ferrierite (Si/Al = 6.2), mordenite (Si/Al = 5.3), Zeolite L (Si/Al = 3.0) and Zeolite Y (Si/Al = 2.8) were also investigated. They found that the maximum activity was obtained on Cu-ZSM-5 catalyst and the lowest activity was on Cu-Y under the same conditions. Delahay et al. [24] and Corma et al. [25] also reported that a similar catalytic activity for NO_x reduction was obtained on Cu-Beta zeolite as compared with Cu-ZSM-5. In this work, we found that Cu-Al-MCM-41 also showed an activity in NO_x reduction by ethylene in the presence of excess oxygen, but the activity was slightly lower than that of Cu-ZSM-5. However, on the Ce^{3+} promoted Cu-Al-

MCM-41 catalyst, we obtained 38% NO_x conversion at 550 °C (Fig. 1), which was close to the maximum value (ca. 40%) on the Cu-ZSM-5 catalyst [11, 16] under similar conditions. The maximum NO_x conversion on the Cu-ZSM-5 was obtained at a lower temperature (250 °C), but Ce-Cu-Al-MCM-41 catalyst had a wider window of the operation temperature (i.e., a window of 200 °C vs. 120 °C at NO_x conversion > 25%, as shown in Fig. 1). Like Cu-ZSM-5, when 5% water vapor and 500 ppm SO_2 were added to reaction gases, the NO_x conversion was found to decrease from 36.0% to 23.8% at 500 °C on the Ce-Cu-Al-MCM-41 catalyst. However, the deactivation by H_2O and SO_2 was less severe compared to that for Cu-ZSM-5.

H_2-TPR and XRD results showed that the copper in the Cu-Al-MCM-41 and Ce-Cu-Al-MCM-41 was mainly present in the form of isolated Cu^{2+} ions. Cu^{2+} ions could be partially reduced to Cu^{+} ions when the samples were treated at high temperatures. Almost no CuO aggregates were detected in the two catalysts. This is consistent with the results obtained in other zeolites (e.g., ZSM-5, Beta zeolite, etc. [5, 6, 24]) that were underexchanged by Cu^{2+}. The isolated Cu^{2+} ions may play an important role in the SCR reaction of NO_x by ethylene. Several authors have claimed that the active species for SCR reaction of NO_x may involve a Cu^{2+}/Cu^{+} redox cycle in Cu^{2+}-exchanged zeolites [24-27]. In the presence of hydrocarbon (e.g., C_2H_4, C_3H_6, C_3H_8, etc.), the Cu^{2+} would be reduced to Cu^{+} and then Cu^{+} was oxidized back to Cu^{2+} by NO_x, thus completing the catalytic cycle. The X-ray absorption near edge structure (XANES) study of Liu and Robota reported that a significant proportion of copper was in the form of Cu^{+} in the presence of propylene (one of the selective reducing agents), even in a large excess of oxygen. Furthermore, the concentration of cuprous ions followed the same trend with temperature as that of NO_x conversion in the reaction. But the use of non-selective reducing agent (e.g., methane) did not lead to the formation of Cu^{+}. Hence, they concluded that

cuprous ions are essential for this reaction. Kutyrev et al. [27] also demonstrated a close correlation between the catalytic activity and the concentration of isolated Cu^{2+} by a series of FTIR study. However, more recently, Haller and coworkers [28] used *in situ* XANES analysis together with comparison of the catalytic behaviors of Cu-ZSM-5 with CuO/Al_2O_3 and CuO/SiO_2 systems and indicated that the rate limiting step of the reaction took place on cupic oxides. They suggested that zeolite supports did not play an essential role in the reaction and that the mechanism might not involve a Cu^{2+}/Cu^{+} redox cycle. Their conclusions were based on the fact that the CuO/Al_2O_3 sample showed a higher activity in the reduction of nitric oxides than the Cu-ZSM-5 under their experimental conditions. On the other hand, reports also exist showing that Cu-ZSM-5 (with high exchange, e.g., 80-100%) was more active than CuO doped Al_2O_3 [4-6, 16]. In this work, only isolated Cu^{2+} and Cu^{+} ions were detected in Cu-Al-MCM-41 and Ce-Cu-MCM-41 catalysts, suggesting that CuO aggregates may not play an important role in this reaction on these two catalysts. After some cerium ions were introduced into Cu-Al-MCM-41, copper ions in the molecular sieve become more easily reducible by H_2. This may be related to the increase of catalytic activity of NO_x reduction by ethylene.

5. Conclusions

Both Cu-Al-MCM-41 and Ce-Cu-Al-MCM-41 were found to be active in the reduction of NO_x to N_2 by ethylene in the presence of excess oxygen. Due to the interaction between cerium and copper, the copper ions in the Ce-Cu-Al-MCM-41 could be reduced by H_2 more easily than those in the Cu-Al-MCM-41. The former also showed a higher NO_x conversion than the latter in the temperature range of 250-600 ^{o}C. In the copper ion-exchanged

Al-MCM-41 catalysts, the copper species were mainly present in the form of isolated Cu^{2+} ions, which may play an important role in the selective catalytic reduction of NO_x to N_2.

References

[1] B.K. Cho, J. Catal., 142 (1993) 418.

[2] M. Iwamoto, "Symposium on Catalytic Technology for Removal of Nitrogen Oxides", pp. 17-22, Catal. Soc. Japan (1990).

[3] W. Held, A. Konig, T. Richter and L. Puppe, SAE Paper 900, 469 (1990).

[4] M. Shelf, Chem. Rev., 95 (1995) 209.

[5] M.D. Amiridis, T. Zhang and R.J. Farrauto, Appl. Catal. B, 10 (1996) 203.

[6] A. Fritz and V. Pitchon, Appl. Catal. B, 13 (1997) 1.

[7] F. Witzel, G.A. Sill and W.K. Hall, J. Catal., 149 (1994) 229.

[8] Y. Li and J.N. Armor, J. Catal., 150 (1994) 376.

[9] Y. Li and J.N. Armor, Appl. Catal. B, 1 (1992) L31.

[10] R.T. Yang and W.B. Li, J. Catal., 155 (1995) 414.

[11] W. Li, M. Sirilumpen, R.T. Yang, Appl. Catal. B, 11 (1997) 347.

[12] H. Hamada, Y. Kinataichi, M. Sasaki and T. Ito, Appl. Catal., 75 (1991) L1.

[13] R. Burch, P.J. Millington and A.P. Walker, Appl. Catal. B, 4 (1994) 65.

[14] X. Feng and W. K. Hall, J. Catal., 166 (1997) 368.

[15] H.Y. Chen and W. M. H. Sachtler, Catal. Lett., 50 (1998) 125.

[16] M. Iwamoto and N. Mizuno, Proc. Inst. Mech. Eng., Part D: J. Automobil Eng., 207 (1993) 23.

[17] C.T. Kresge, M.E. Leonwicz, W.J. Roth, J.C. Vartuli and J.C. Beck, Nature, 359

(1992) 710.

[18] J.S. Beck, J.C. Vartuli, W.J. Roth, M.E. Leonowicz, C.T. Kresge, K.D. Schmitt, C.T.W. Chu, D.H. Olson, E.W. Sheppard, S.B. McCullen, J.B. Higgins and J.L. Schlenker, J. Am. Chem. Soc., 114 (1992) 10834.

[19] R.T. Yang, T.J. Pinnavaia, W. Li and W. Zhang, J. Catal., 172 (1997) 488.

[20] R.Q. Long and R.T. Yang, Catal. Lett., in press.

[21] X.S. Zhao, G.Q. Lu and G.J. Millar, Ind. Eng. Chem. Res., 35 (1996) 2075.

[22] R.B. Borade and A. Clearfield, Catal. Lett., 31 (1995) 267.

[23] P.T. Tanev and L.T. Vlaev, J. Colloid Interface Sci., 160 (1993) 110.

[24] G. Delahay, B. Coq and L. Broussous, Appl. Catal. B, 12 (1997) 49.

[25] A. Corma, V. Fornes and E. Palomares, Appl. Catal. B, 11 (1997) 233.

[26] D.J. Liu and H.J. Robota, Appl. Catal. B, 4 (1994) 155.

[27] M.Y. Kutyrev, A.A. Ukharsky, A.N. Ilichev and V.A. Matyshak, Proc. 1st Int. Cong. on Environ. Catal., Pisa, 1995, p. 311.

[28] C. Marquez-Alvarez, I. Rodriguez-Ramos, A. Guerrero-Ruiz, G.L. Haller and M. Fernandez- Garcia, J. Am. Chem. Soc., 119 (1997) 2905.

Table 1 Main characteristics of the catalysts

Sample	BET Specific Surface Area (m^2/g)	Pore Volume (cm^3/g)	Pore Diameter (nm)	H_2/Cu (TPR) (mol/mol)	
				1^{st} peak	2^{nd} peak
Al-MCM-41	917	1.05	4.3	—	—
Ce-Al-MCM-41	904	1.09	4.2	—	—
Cu-Al-MCM-41	885	1.03	4.1	0.41	0.51
Ce-Cu-Al-MCM-41	871	1.03	4.8	0.36	0.49

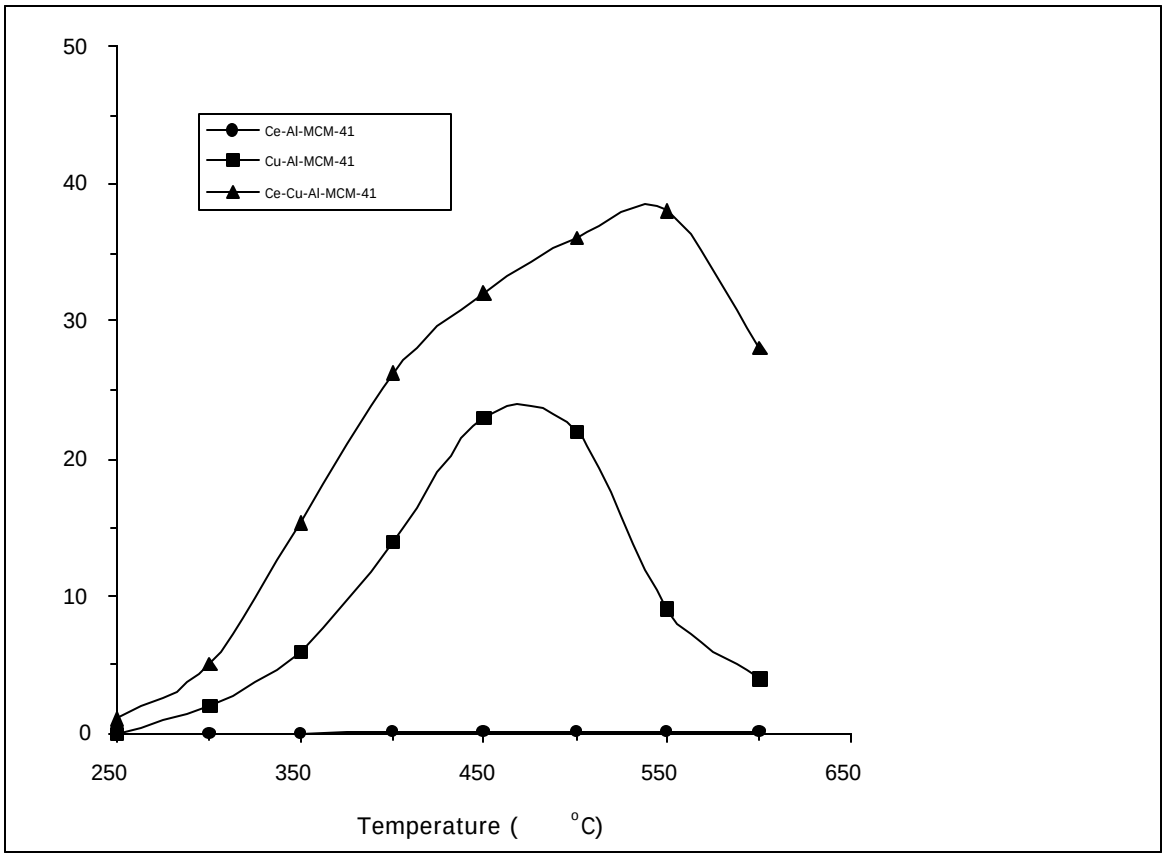

Fig.1 Conversions of NO_x for SCR reaction on (a) Ce-Al-MCM-41, (b) Cu-Al-MCM-41 and (c) Ce-Cu-Al-MCM-41. Reaction conditions: catalyst = 0.5 g, [NO] = [C_2H_4] = 1000 ppm, [O_2] = 2%, He = balance, total flow rate = 250 ml/min, and space velocity ≈ 7500 h^{-1} .

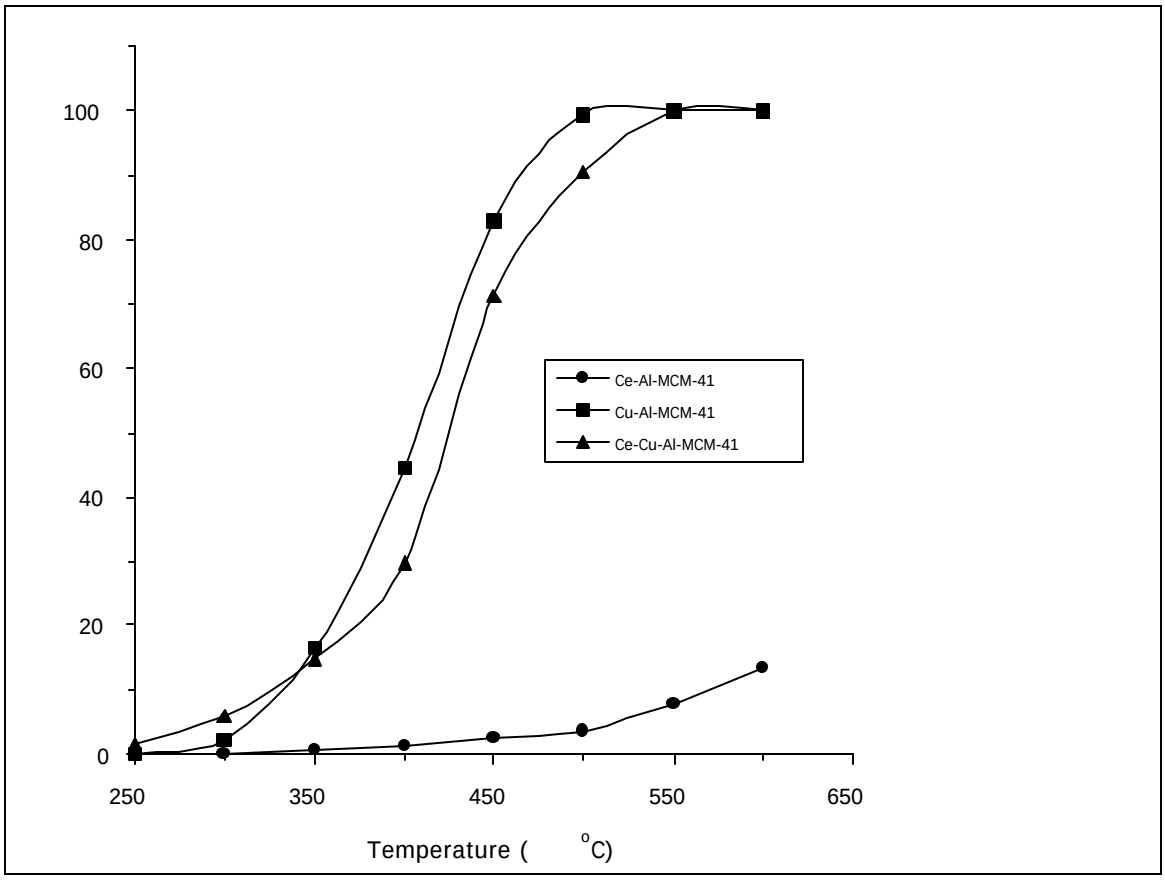

Fig. 2 Conversions of C_2H_4 for SCR reaction on (a) Ce-Al-MCM-41, (b) Cu-Al-MCM-41 and (c) Ce-Cu-Al-MCM-41. Reaction conditions are the same as in Fig. 1.

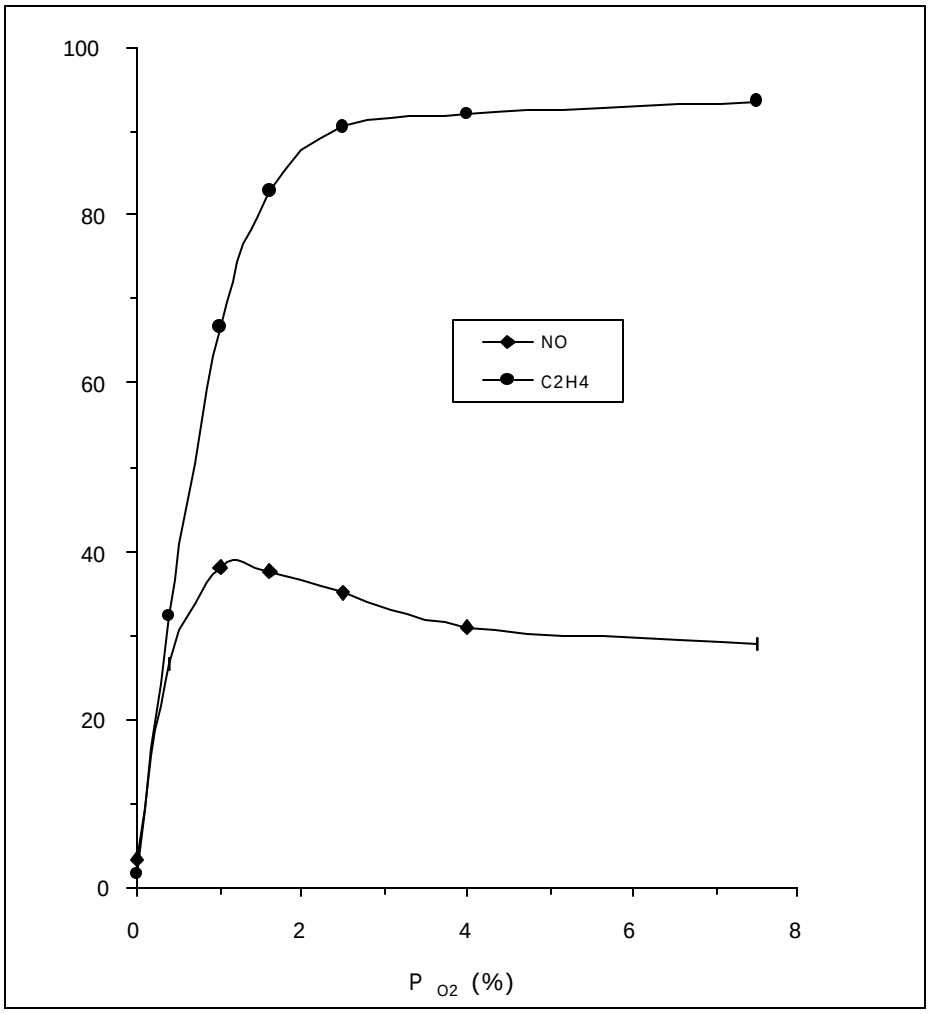

Fig. 3 Effect of O_2 concentration on SCR activity on Ce-Cu-Al-MCM-41 catalyst. Reaction conditions: temperature = 500 °C, catalyst = 0.5 g, [NO] = [C_2H_4] = 1000 ppm, He = balance, total flow rate = 250 ml/min, and space velocity ≈ 7500 h^{-1} .

CHAPTER THREE

Pt/MCM-41 catalyst for selective catalytic reduction of nitric oxide with hydrocarbons in the presence of excess oxygen

1. Introduction

Removal of NO_x ($NO + NO_2$) from exhaust gases is a challenging subject that has been extensively studied in recent years. The selective catalytic reduction (SCR) of NO_x is one of the most effective means. For large power plants, V_2O_5/TiO_2 has been the main commercial catalyst for SCR with NH_3 for stationary sources [1]. However, for diesel- and gasoline-fueled engines in vehicles, the use of NH_3-based SCR technologies is not practical because of the high cost and NH_3 handling problems. The three-way catalyst has been used commercially in gasoline engines for reduction NO to N_2 by carbon monoxide and hydrocarbons under rich-burn conditions, but it becomes ineffective in the presence of excess oxygen [2]. The first catalyst found to be active for selective catalytic reduction of NO by hydrocarbons in the presence of excess oxygen was copper exchanged ZSM-5, reported in 1990 by Iwamoto et al.[3] and Held et al.[4]. A large number of catalysts have been found to be active for these reactions since 1990, such as Cu-ZSM-5 [3-6], Co-ZSM-5 and Co-Ferrierite [7-9], Co/Al_2O_3 [10], Ce-ZSM-5 [11], Cu^{2+}-exchanged pillared clay [12, 13], Fe-ZSM-5 [14], Pt-ZSM-5 [15-17], Rh-ZSM-5 [17], Pt/Al_2O_3 [18-20], and supported Ag [21]. Although Cu-ZSM-5 is very active and the most intensively studied catalyst, it suffers from severe deactivation in engine tests, mainly due to H_2O and SO_2 [22, 23]. By comparison, Pt-ZSM-5 was found to be more active than Cu-ZSM-5 and Fe-MOR at lower temperatures (127-277 °C) [15] and the catalysts containing Pt were stable in real diesel exhaust [24]. They appeared to be one of the most promising catalysts.

MCM-41, a new member of the zeolite family, shows a regular hexagonal array of uniform pore openings with pore dimensions between 1.5 and 10 nm [25, 26]. Because it has high thermal stability, high BET surface areas and large pore volumes, MCM-41 has already attracted considerable interests in recent years [27]. It has been studied as catalysts, support and sorbents [27]. Corma and co-workers [28] reported a good catalytic activity for MCM-41 in selective oxidation of hex-1-ene with H_2O_2, and norbornene with terbutylhydroperoxide on Ti-MCM-41 catalyst. Fe-Al-MCM-41 were also reported by Yang et al. [29] as a good catalyst for selective catalytic reduction of NO with NH_3. In this work, we investigated the activity of platinum doped MCM-41 in SCR of NO with methane, ethylene, propane and propylene in the presence of excess oxygen. The effects of oxygen, water vapor and sulfur dioxide on SCR activity were also studied.

2. Experimental

Pure silica MCM-41 was synthesized according to the procedure given by Kim et al. [30]. 30.1 ml sodium silicate solution (containing 14% of NaOH and 27% of SiO_2, Aldrich) was dropwise added to a three-neck flask containing a mixture of 41.3 ml cetyltrimethylammonium chloride (CTMACl, 25 wt% in water, Aldrich), 0.6 ml 28 wt% NH_3 aqueous solution (J.T. Baker) and deionized water, with constant stirring at room temperature. The resulting gel mixture had the following molar composition: 1 SiO_2 : 0.166 CTMACl : 0.388 Na_2O : 0.0247 NH_4OH : 40 H_2O. After stirring for 1 h, the mixture was heated to 97 °C for 24 h, then cooled down to room temperature and the pH was adjusted to 10.2 by adding 2N

HNO_3. The reaction mixture (pH=10.2) was heated to 97 °C again for 24 h. This procedure of pH adjustment and subsequent heating (for 24 h duration) was repeated twice. Finally, the product was filtered, washed with deionized water, dried at 110 °C for 12 h and then calcined at 560 °C for 10 h in a flow of air (150 ml/min). 0.5-5 wt% Pt/MCM-41 catalysts were prepared by using the incipient wetness impregnation method with hydrogen hexachloroplatinate (IV) hydrate (99.9%, Aldrich) as the platinum precursor. After calcination at 500 °C for 4 h in air, the samples were crushed to 60-100 mesh.

The powder X-ray diffraction (XRD) measurement was carried out with a Rigaku Rotaflex D/Max-C system with CuK_α (λ = 0.1543 nm) radiation. The samples were loaded on a sample holder with a depth of 1 mm. XRD patterns were recorded in the ranges of 2θ = 1-10° and 30-70°. A Micromeritics ASAP 2010 micropore size analyzer was used to measure the N_2 adsorption isotherm of the samples at liquid N_2 temperature (-196 °C). The specific surface areas of the samples were determined from the linear portion of the BET plots (P/P_0 = 0.05-0.20). The pore size distribution was calculated from the desorption branch of the N_2 adsorption isotherm using the Barrett-Joyner-Halenda (BJH) Formula, as suggested by Tanev and Vlaev [31], because the desorption branch can provide more information about the degree of blocking than the adsorption branch hence the best results were obtained from the BJH formula. Prior to the surface area and pore size distribution measurements, the samples were dehydrated at 350 °C for 4 h.

The dispersions of Pt in the Pt/MCM-41 catalysts were measured by CO chemisorption on a thermogravimetric analyzer (TGA, Cahn 2000 System 113). Prior to CO chemisorption, the samples were first reduced by H_2 (5.34% H_2 in N_2) at 400 °C for 5 h or

more, followed by cooling to room temperature in He flow. Chemisorption of CO was performed at room temperature (with 1.03% CO in He). Equilibrium was assumed when no further weight gain was observed. Based on the amount of CO adsorbed and assuming 1:1 ratio for Pt_s:CO, Pt dispersions were obtained.

The SCR activity measurement was carried out in a fixed-bed quartz reactor. The reaction temperature was controlled by an Omega (CN-2010) programmable temperature controller. 0.1 g or 0.2 g of sample was used in this work. The typical reactant gas composition was as follows: 1000 ppm NO, 1000-3000 ppm hydrocarbons (CH_4, C_2H_4, C_3H_8 and C_3H_6), 0-7.8% O_2, 500 ppm SO_2 (when used), 2.4% water vapor (when used), and balance He. The total flow rate was 250 ml/min (ambient conditions). The premixed gases (1.01% NO in He, 1.05% CH_4 in He, 1.04% C_2H_4 in He, 1.07% C_3H_6 in He, 0.98% C_3H_8 in He and 0.99% SO_2 in He) were supplied by Matheson Company. The NO and NO_2 concentrations were continuously monitored by a chemiluminescent NO/NO_x analyzer (Thermo Electro Corporation, Model 10). The other effluent gases were analyzed by a gas chromatograph (Shimadzu, 14A) at 50 °C with 5A molecular sieve column for O_2, N_2 , CH_4 and CO, and Porapak Q column for CO_2, N_2O, C_2H_4, C_3H_6 and C_3H_8. Other details of the SCR reaction system were described elsewhere [32].

3. Results and Discussion

The XRD pattern of pure MCM-41 consisted of one very strong peak at $2\theta = 2.14°$ and three weak peaks at $2\theta = 3.77°$, 4.31° and 5.79°, which can be indexed, respectively, to

(100), (110), (200) and (210) diffraction peaks characteristic of a hexagonal structure of MCM-41 [25, 26, 30]. According to the value of d_{100} (d_{100} = 4.14 nm), the unit cell dimension (a = 4.78 nm) was calculated by using the formula: $a = 2d_{100}/\sqrt{3}$. After platinum dopings on the MCM-41 sample, the XRD patterns were essentially unchanged, indicating that the incipient wetness impregnation process did not alter the framework structure of this zeolite. The platinum metal phase, with peaks at 2θ of 39.73°, 46.24° and 67.41°, could also be identified in the XRD patterns of the Pt/MCM-41 catalysts. These three peaks were reflections of, respectively, (111), (200) and (220) faces of the cubic platinum metal structure. With increasing amount of platinum, the intensities of these peaks were seen to increase. No platinum oxide phase was detected, whose three strongest peaks would have been found at 2θ of 34.8°, 42.5° and 54.9°. This was most probably due to its good dispersion on the catalysts. The BET specific surface area, pore volume, average pore diameter, platinum dispersion of the Pt/MCM-41 catalysts are summarized in Table 1. The Pt/MCM-41 catalysts were found to have narrow pore size distributions with pore sizes near 3.8 nm, high BET surface areas(> 900 m^2/g) and large pore volumes(> 1.00 cm^3/g). The Pt dispersion obtained by CO chemisorption was between 54% and 24% on the 0.5-5% Pt/MCM-41 catalysts, with higher dispersions for lower Pt amounts.

The catalytic performance of 0.5-5 % Pt/MCM-41 for the reduction of NO with C_3H_6 is shown in Table 2. At lower temperatures(below 200 °C), NO conversion and C_3H_6 conversion were small. With increasing temperature, NO conversion was found to increase at first, passing through a maximum, then decreased at higher temperatures. The maximum NO conversion appeared at the temperature at which propylene conversion reached 100%. Carbon

dioxide was the only product (beside water) of propylene oxidation. The N balance and C balance were above 94% in this work. Similar to other platinum doped or exchanged catalysts reported in the literature, N_2O was the main product. This may be related to the fact that platinum is a poor N_2O decomposition catalyst [20,33]. When the platinum amount increased from 0.5% to 5%, the peak NO conversion temperature decreased from 275 °C to 250 °C. At high temperatures, the decrease in NO conversion was due to the oxidation of C_3H_6 by O_2. The turnover frequencies (TOF) for the conversion of NO, defined as the number of NO molecules converted per surface Pt atom per second, are also given in Table 2. With the increase of platinum amount, the maximum TOF was found to decrease. The steady-state NO reduction rate (mmol/g·h) was calculated as [8]

$$\text{NO reduction rate} = -d[NO]/dt = F_0X / w \qquad (1)$$

where F_0 was inlet molar flow rate of NO, X was NO conversion and w was weight of the catalyst. The maximum NO reduction rate on these Pt/MCM-41 catalysts were 3.6-4.3 mmol/g·h at 275 or 250 °C, which was higher than 2.8 mmol/ gh obtained on 1% Pt/Al_2O_3 catalyst [20] under similar conditions. Hamada et al. [18] reported that the activity for SCR decreased significantly when alumina was replaced by silica as the support for Pt. Pt supported on ZSM-5 also showed SCR activity [15, 17]. It was claimed that Pt was ion-exchanged on ZSM-5 [15, 17]. However, characterization of these materials has indicated that in many case Pt exists on the exterior surface of the ZSM-5 crystals as fine metallic particles, and hence was not an effective support [34]. This indicates that the nature of the support plays an important role in the activity of NO reduction with hydrocarbon on platinum. The high activity obtained on

the Pt/MCM-41 catalysts was likely due to the large pores and high surface area of MCM-41. Pore diffusion limitation is known to be significant for the SCR reaction [29].

It is well known that oxygen is important in SCR reactions of NO both by hydrocarbons [34] and by NH_3 [1]. The effect of O_2 on SCR by C_3H_6 over 1% Pt/MCM-41 at 250 °C was studied. In the absence of O_2, almost no activity was obtained. When 0.5% of O_2 was added to the reactant gas mixture, NO conversion was found to increase significantly to 88% and C_3H_6 conversion also reached 100% at the same temperature. After that, NO conversion decreased slightly with the increase of O_2 concentration. It is known that reduced platinum atoms play an important role for NO conversion [34, 35]. Burch and Watling reported that about 14% of platinum atoms on the Pt/Al_2O_3 catalyst surface were in the reduced form under the reaction conditions and that NO did not convert to N_2 on a completely oxidized, supported platinum catalyst [19, 35]. In this work, after the Pt/MCM-41 catalysts were calcined at 500°C in air (21% of O_2), the platinum metal phase was still detected by XRD. The XRD result combined with the high dispersions were indirect evidence for the high probability that there existed reduced Pt atoms on the surface. The reduced platinum atoms could be the active sites for NO reduction. The role of oxygen was attributed to its reaction with hydrocarbon fragments left on the Pt sites and thus prevention of the deactivation of the active sites by coke formation [34].

In order to compare directly the effect of different hydrocarbons on SCR activity of NO, we also studied the catalytic performance on the 1% Pt/MCM-41 sample using CH_4, C_2H_4 and C_3H_8 as reductants at the same carbon concentration condition, i.e., 3000 ppm of CH_4, 1500 ppm of C_2H_4 and 1000 ppm of C_3H_8, as compared with 1000 ppm of C_3H_6. For

CH_4 and C_3H_8, no or little activity for NO reduction was found on the 1% Pt/MCM-41 catalyst in the temperature range of 150-450 °C. At higher temperatures, only a small amount of CH_4 was oxidized to CO_2 by O_2, while a large amount of C_3H_8 was converted to CO_2 by O_2. By comparison, a very high activity was obtained when C_2H_4 and C_3H_6 were used as the reductants. The maximum NO conversion reached 81% at 225 °C. This indicated that C_2H_4 and C_3H_6 were excellent reductants but CH_4 and C_3H_8 were poor reductants for SCR of NO over the Pt/MCM-41 catalyst. Similar phenomenon was observed on Pt/Al_2O_3 and Pt/SiO_2 catalysts [36]. This difference is related to the nature of these hydrocarbons. Ethylene and propylene have a C=C double bond and are easy to adsorb on platinum atoms and thus result in a high converage of these alkene species. So the surface is readily reduced to Pt atoms. However, methane and propane are saturated hydrocarbons and thus must have the C-H bond broken to chemisorb on the Pt surface. So adsorbed oxygen is the predominant surface species [36]. Because the C-H bond energy in the CH_4 molecule (105 kcal/mol) is larger than that in C_3H_8 molecule (95 kcal/mol), a higher C_3H_8 conversion was obtained using C_3H_8 as the reductant than that using CH_4 as the reductant in the high temperature range. It is not surprising that Pt and PtO might have different catalytic properties for SCR reaction of NO on platinum doped catalysts. Ethylene and Propylene are better reductants than methane and propane on the Pt/MCM-41 catalyst.

The effect of H_2O and SO_2 on SCR activity of NO with C_3H_6 on 1% Pt/MCM-41 catalyst is studied. The result exhibited that the Pt/MCM-41 catalyst was a stable catalyst. After being on stream for 10 h at 225 °C, under the conditions of 1000 ppm NO, 1000 ppm C_3H_6, 2% of O_2, He as balance and 250 ml/min of total flow rate, NO conversion remained at 80-

81%. When 2.4% water vapor and 500 ppm SO_2 were added to the reactant gas, the catalytic performance remained unchanged in the following 4 h at 225 °C.

4. Conclusions

0.5-5 wt% Pt/MCM-41 catalysts were prepared and studied for the selective catalytic reduction of NO with CH_4, C_2H_4, C_3H_6 and C_3H_8 in the presence of excess oxygen. The catalysts had high BET surface areas (> 900 m^2/g) and large pore volumes(> 1.00 cm^3/g). Platinum metal particles were detected in these catalysts at room temperature by XRD. A high activity for NO reduction was obtained when C_2H_4 or C_3H_6 was used as the reductant and the maximum NO reduction rate reached 4.3 mmol/g·h under the conditions of 1000 ppm NO, 1000 ppm C_3H_6, 2% of O_2 and He as balance; but no or little activity was found when CH_4 or C_3H_8 was used. This difference was related to the different nature of these hydrocarbons. The Pt/MCM-41 catalyst showed a good stability. H_2O and SO_2 did not cause deactivation of the catalyst.

References:

[1] H. Bosch and F. Janssen, Catal. Today, 2 (1988) 369.

[2] B.K. Cho, J. Catal., 142 (1993) 418.

[3] M. Iwamoto, "Symposium on Catalytic Technology for Removal of Nitrogen Oxides", pp. 17-22, Catal. Soc. Japan (1990).

[4] W. Held, A. Konig, T. Richter and L. Puppe, SAE Paper 900, 469 (1990).

[5] J. Valyon and W.K. Hall., J. Catal., 143 (1993) 520.

[6] A.P. Ansell, A.F. Diwell, S.E. Colunski, J. W. Hayes, R.R. Rajaran, T.J. Truex and A.P. Walker, Appl. Catal. B, 2 (1993) 101.

[7] F. Witzel, G.A. Sill and W.K. Hall, J. Catal., 149 (1994) 229.

[8] Y. Li and J.N. Armor, J. Catal., 150 (1994) 376.

[9] Y. Li and J.N. Armor, Appl. Catal. B, 1 (1992) L31.

[10] J. Y. Yan, M.C. Kung, W.M.H. Sachtler and H.H. Kung, J. Catal., 172 (1997) 178.

[11] M. Misono and K.Konodo, Chem. Lett., (1991) 1001.

[12] R.T. Yang and W.B. Li, J. Catal., 155 (1995) 414.

[13] W. Li, M. Sirilumpen, R.T. Yang, Appl. Catal. B, 11 (1997) 347.

[14] X. Feng and W.K Hall, J. Catal., 166 (1997) 368.

[15] H. Hirabayashi, H. Yahiro, N. Mizuno and M. Iwamoto, Chem. Lett., (1992) 2235.

[16] M. Iwamoto, H. Yahiro, H.K. Shin, M. Watababe, J. Guo, M. Konno, T. Chikahisa and T. Murayama, Appl. Catal. B, 5 (1994) L1.

[17] R. Burch and S. Scire, Appl. Catal. B, 3 (1994) 295.

[18] H. Hamada, Y. Kinataichi, M. Sasaki and T. Ito, Appl. Catal., 75 (1991) L1.

[19] R. Burch, P.J. Millington and A.P. Walker, Appl. Catal. B, 4 (1994) 65.

[20] R. Burch and T.C. Watling, Appl. Catal. B, 11 (1997) 207.

[21] K.A. Bethke and H.H. Kung, J. Catal., 172 (1997) 93.

[22] J.N. Armor, Appl. Catal. B, 4 (1994) N18.

[23] M.J. Heimrich and M.L. Deviney, SAE Paper 930, 736 (1994).

[24] A. Obuchi, A. Ohi, M. Nakamura, A. Ogata, K. Mizuno and H. Ohuchi, Appl. Catal.

B, 2 (1993) 71.

[25] C.T. Kresge, M.E. Leonwicz, W.J. Roth, J.C. Vartuli and J.C. Beck, Nature, 359 (1992) 710.

[26] J.S. Beck, J.C. Vartuli, W.J. Roth, M.E. Leonowicz, C.T. Kresge, K.D. Schmitt, C.T.W. Chu, D.H. Olson, E.W. Sheppard, S.B. McCullen, J.B. Higgins and J.L. Schlenker, J. Am. Chem. Soc., 114 (1992) 10834.

[27] X.S. Zhao, G.Q. Lu and G. J. Millar, Ind. Eng. Chem. Res., 35 (1996) 2075.

[28] A. Corma, M.T. Navarro and J. Perez Pariente, J. Chem. Soc., Chem. Commun., (1994) 147.

[29] R.T. Yang, T.J. Pinnavaia, W. Li and W. Zhang, J. Catal., in press, 1997.

[30] J.M. Kim, J.H. Kwak, S. Jun and R. Ryoo, J. Phys. Chem., 99 (1995) 16742.

[31] P.T. Tanev and L.T. Vlaev, J. Colloid Interface Sci., 160 (1993) 110.

[32] R.T. Yang, J.P. Chen, E.S. Kikkinides, L.S. Cheng and J.E. Cichanowicz, Ind. Eng. Chem. Res., 31 (1992) 144.

[33] Y. Li and J.N. Armor, Appl. Catal. B, 1 (1992) L21.

[34] M.D. Amiridis, T. Zhang and R.J. Farrauto, Appl. Catal. B, 10 (1996) 203.

[35] R. Burch and T.C. Watling, Catal. Lett., 37 (1996) 51.

[36] R. Burch and T.C. Watling, Catal. Lett., 43 (1997) 19.

Table 1 Platium dispersions and pore structure parameters of the Pt/MCM-41 catalysts

Catalyst	BET Specific Surface Area (m^2/g)	Pore Volume (cm^3/g)	Pore Diameter (nm)	CO (mg) /gcat	Pt dispersion (%)
0.5% Pt/MCM-41	947	1.14	3.80	0.38	54
1% Pt/MCM-41	928	1.08	3.73	0.53	37
2% Pt/MCM-41	943	1.13	3.81	1.00	35
5% Pt/MCM-41	908	1.10	3.87	1.71	24

Table 2 Catalytic performance of Pt/MCM-41 for selective catalytic reduction of NO with C_3H_6 at different temperatures

Catalyst	Temp. (°C)	NO Conv. (%)	NO Conv. to N_2 (%)	NO Conv. to N_2O (%)	TOF/10^{-3} (s^{-1})	C_3H_6 Conv. (%)
0.5% Pt/MCM-41	200	2.0	2.0	0	2.7	1
	225	6.0	3.0	3.0	8.1	3.1
	250	17.0	6.2	10.8	23	11.7
	275	54.0	18.7	35.3	73	100
	300	37.0	8.5	28.5	50	100
1.0% Pt/MCM-41	200	4.0	2.2	1.8	3.9	4.0
	225	8.0	4.4	3.6	7.9	10.2
	250	61.0	16.9	44.1	60	100
	275	49.0	15.2	33.8	48	100
	300	36.0	11.6	24.4	35	100
2.0% Pt/MCM-41	200	13.0	7.2	5.8	6.8	14.5
	225	33.0	13.8	19.2	17	27.0
	250	59.0	15.2	43.8	31	100
	275	48.0	13.0	35.0	25	100
	300	37.0	10.0	27.0	19	100
5.0% Pt/MCM-41	200	7.0	1.3	5.7	2.1	3.3
	225	20.0	6.7	13.3	6.1	13.2
	250	63.6	15.4	48.2	19	100
	275	61.0	13.2	47.8	18	100
	300	47.0	10.6	36.4	14	100

Conditions: 0.1 g of catalyst, NO = 1000 ppm, C_3H_6 = 1000 ppm, O_2 = 2%, He = balance, total flow rate = 250 ml/min.

TOF (turnover frequency) is defined as the number of NO molecules converted per surface Pt atom per second.

CHAPTER FOUR

In Situ FT-IR Study of Rh-Al-MCM-41 Catalyst for the Selective Catalytic Reduction of Nitric Oxide with Propylene in the Presence of Excess Oxygen

Introduction

Removal of nitrogen oxides (NO_x, x = 1, 2) from exhaust gases has been a challenging problem in recent years. Selective catalytic reduction (SCR) of NO_x by hydrocarbons in the presence of excess oxygen has been extensively studied.[1,2] Supported Pt-group metals have been reported to be active at lower temperatures and are stable in the presence of water vapor and sulfur dioxide.[1-9] Platinum, iridium, palladium, rhodium and ruthenium supported on Al_2O_3, TiO_2, SiO_2, ZrO_2, and ZSM-5 have been studied.[3-8] More recently, MCM-41 as a support and ion-exchanged MCM-41 have been studied in our laboratory[9] for the SCR reaction. Both ZSM-5 and MCM-41 have channel-type pores, however, the pores are much bigger in the MCM-41 catalysts, i.e., 0.5-0.6 nm in ZSM-5 vs. 3-4 nm in MCM-41. Hence the mass transfer resistance is considerably lower in the MCM-41 catalysts. Among various noble metals doped on Al_2O_3, Pt was reported to be the most active and resistant to H_2O and SO_2, but it produces substantial amount of N_2O. By comparison, Rh/Al_2O_3 has the highest product selectivity for N_2.[5] These different behaviors may be related to the different characteristics of the two metals and thus two different reaction pathways in the SCR reaction. For Pt supported catalysts, e.g., Pt/Al_2O_3 and Pt/ZSM-5, the reaction mechanism has been studied by TAP

(temporal analysis of products) and FT-IR techniques.[8,10] It has been generally accepted that the reaction path for reduction of nitric oxide involves a two-step process in which the NO molecules are decomposed to N and O atoms on the reduced platinum sites, then the N atom combines another N atom or a NO molecule to produce N_2 or N_2O. The oxidized Pt sites are regenerated by reduction with hydrocarbons (e.g., C_3H_6).[8,10,11] However, few studies on SCR on Rh supported catalysts have been reported and the mechanism for NO reduction on Rh catalysts is still unclear.[2,7,12].

In this work, we first report the activities and product selectivities of Rh-exchanged Al-MCM-41 for SCR of NO by propylene in the presence of excess oxygen. The mechanism was studied by focusing on the surface adspecies of the catalyst by *in situ* FT-IR spectroscopy under reaction conditions. MCM-41 was chosen for this study because it has high thermal stability, high BET surface area and large pore volume. It has already attracted considerable interests in resent years. It has been studied as catalysts, support and sorbents.[13-16] In our previous study, platinum doped MCM-41 catalyst showed higher specific activity than Pt/Al_2O_3 for the SCR reaction.[9] The present study shows that the Rh-exchanged Al-MCM-41 catalyst is more active and selective for N_2 than the Pt doped MCM-41 catalyst. It is also shown that N_2 and N_2O originate mainly from the reaction between $Rh\text{-}NO^+$ and propylene adspecies.

Experimental Section

Catalyst Preparation and Characterization. Al-MCM-41 (Si/Al=10) was synthesized according to the procedure given by Borade and Clearfield.[17] Fumed silica (99.8%, Aldrich), tetramethylammonium hydroxide pentahydrate (TMAOH, 97%, Aldrich), 25 wt.% cetyltrimethylammonium chloride (CTMACl) in water (Aldrich), $Al[C_2H_5CH(CH_3)O]_3$ (97%, Aldrich) and NaOH (98.1%, Fisher) were used as source materials for preparing Al-MCM-41. Solution A was prepared by dissolving 1.325 g TMAOH in 100 ml deionized water and then adding 5 g fumed silica. Solution B was obtained by dissolving 0.72 g NaOH in deionized water and adding 25 ml CTMACl followed by adding 2.19 ml $Al[C_2H_5CH(CH_3)O]_3$ at room temperature. The two solutions were stirred for 10-15 min, then solution A was added to solution B. The reaction mixture had the following chemical composition $1SiO_2$-$0.05Al_2O_3$-$0.23CTMACl$-$0.11Na_2O$-$0.089TMAOH$-$125H_2O$. After being stirred for 15 min, the mixture was transferred into a 250 ml three-neck flask and was then heated at 100 °C for 48 h. After filtering, the solid was washed, dried and calcined at 560 °C for 10 h in a flow of air (150 ml/min). The XRD pattern of Al-MCM-41 (Fig. 1) was consistent with that reported previously

for Al-MCM-41 molecular sieve[13,17] and all XRD peaks could be indexed on a hexagonal lattice with d_{100} = 3.9 nm.

Rh-exchanged Al-MCM-41 was prepared by using conventional ion exchange procedure. 1 g Al-MCM-41 sample was added to 200 ml 10^{-3} M $Rh(NO_3)_3$ solution at 70 ^oC with constant stirring. The pH value of the solution was adjusted to 6 with NaOH solution in order to maximize the rhodium ion-exchange capacity. A low pH is not favorable for ion exchange because of competition from H^+ and the fact that Rh exists as Rh^{3+}. At high pH Rh would precipitate as $Rh(OH)_3$. The exchange process was carried out for 6 h and repeated three times. After that, the mixture was filtered and washed 5 times with deionized water. The obtained solid sample was first dried at 120 ^oC in air for 12 h, then heated at 400 ^oC for 6 h in a flow of 5.34%H_2/N_2. The rhodium content in the Rh-Al-MCM-41 sample was analyzed by neutron activation analysis and was 3.14% (i.e., 61.7% ion exchange). The Rh dispersion was determined by CO chemisorption[9] and was 93%. The BET surface area, pore volume and average pore size of the Rh-Al-MCM-41 sample measured by N_2 adsorption at -196 ^oC with a Micromeritics ASAP 2010 micropore size analyzer were 952 m^2/g, 1.22 cm^3/g and 4.5 nm, respectively.

Catalytic Performance Measurement. The SCR activity measurement was carried out in a fixed-bed quartz reactor.[9] 0.1 g sample, as particles of 60-100 mesh, was used in this work without any pretreatment. The activity was measured after reaching a "steady state." The typical reactant gas composition was as follows: 1000 ppm NO, 1000 ppm C_3H_6, 2% O_2 and balance He. The total flow rate was 250 ml/min (ambient conditions). The premixed gases (1.01% NO in He and 1.00% C_3H_6 in He) were supplied by Matheson Company. The NO_x concentration was continuously monitored by a chemiluminescent NO/NO_x analyzer (Thermo Electro Corporation, Model 10). The other effluent gases were analyzed by a gas chromatograph (Shimadzu, 14A) at 50 °C with a 5A molecular sieve column for O_2 , N_2 and CO, and a Porapak Q column for CO_2, N_2O and C_3H_6.

FT-IR Study. Infrared spectra were recorded on a Nicolet Impact 400 FT-IR spectrometer with a TGS detector. Self-supporting wafers of 1.3 cm diameter were prepared by pressing 10 mg samples and were loaded into a high temperature IR cell with BaF_2 windows. The wafers could be pretreated *in situ* in the IR cell. The wafers were first treated at 400 ^oC in a flow of He (99.9998%) for 30 min, and then cooled to desired temperatures, i.e., 350, 300, 250, 200, 100 ^oC. At each temperature, the background spectrum was recorded in

flowing He and was subtracted from the sample spectrum that was obtained at the same temperature. Thus the IR absorption features that originated from the structural vibrations of the catalyst were eliminated from the sample spectra. Unless otherwise stated, a standard pretreatment procedure at 350 ^{o}C was performed before gas adsorption. The procedure consisted of oxidizing the sample in flowing O_2 for 10 min followed by purging with He for 15 min, then reducing the sample by H_2 for 10 min and finally flushing in He for 15 min. In the experiment, the IR spectra were recorded by accumulating 100 or 8 scans at a spectral resolution of 4 cm^{-1}. The gas mixtures (i.e., NO/He, C_3H_6/He, NO+O_2/He, C_3H_6+O_2/He, NO+C_3H_6+O_2/He, etc.) had the same concentrations as that used in the activity measurements, i.e., 1000 ppm NO (when used), 1000 ppm C_3H_6 (when used), 2% O_2 (when used) and balance of He. The total gas flow rate was 250 ml/min.

Results and Discussion

Catalytic Performance for SCR Reaction. For pure Al-MCM-41, no NO conversion to N_2 or N_2O was obtained at 200-400 ^{o}C under the reaction conditions (0.1 g sample, 1000 ppm NO, 1000 ppm C_3H_6, 2% O_2 and 250 ml/min of total flow rate). Whereas,

as shown in Table 1, Rh-Al-MCM-41 was active for the SCR reaction. With increasing temperature, the NO conversion increased first, passing through a maximum, then decreased at higher temperatures. The maximum NO conversion appeared at the temperature at which C_3H_6 conversion reached 100%. At high temperatures, the decrease in NO conversion was due to the combustion of C_3H_6 by O_2. Carbon dioxide was the only product (besides water) of propylene oxidation. The nitrogen balance was above 95% in this work. The product selectivity for N_2 was between 60% and 78%. The maximum NO conversion on Rh-Al-MCM-41 catalyst was slightly higher than that on Pt/MCM-41 catalyst (68.2% at 300 ^oC vs. 63.6% at 250 ^oC)[9] under the same reaction conditions. The former also had much higher product selectivities for N_2 than the latter, which is in agreement with the previous result that Rh doped catalysts have higher N_2 selectivities than Pt catalysts.[2] Since Al-MCM-41 was inactive in the SCR reaction, it is clear that rhodium acted as active sites for NO reduction on the Rh-Al-MCM-41 catalyst. The high activity on the catalyst may be attributable to the high rhodium dispersion (93%, obtained by CO chemisorption). It is known that ion exchange can be used to prepare highly dispersed Rh in NaY zeolite.[18]

IR Spectra of NO and NO_2 Adsorption on Rh-Al-MCM-41 Catalyst. The adsorption of NO and NO_2 was studied at 250 ^oC on both oxidized and reduced Rh-Al-MCM-41 by FT-IR spectroscopy. The oxidized Rh-Al-MCM-41 was obtained by calcining the sample at 350 ^oC in a flow of O_2 for 10 min followed by purging with He for 15 min. After the sample was exposed to a flowing NO/He for 10 min at 250 ^oC, three IR bands were observed at 1900, 1634 and 1534 cm^{-1} (Fig. 2a). The band at around 1900 cm^{-1} was always observed on NO adsorbed Rh catalysts. It is attributable to NO adsorbed on the partially oxidized Rh sites, i.e., $Rh\text{-}NO^+$ [7,19-21], which is generated by the donation of the unpaired electron from the $2p\ ^*$ antibonding orbital of the NO molecule to the 4d orbital of rhodium. This results in an increase in the strength of N-O bond and hence the NO molecule associated with Rh^+ sites is more difficult to decompose to N and O atoms than the free NO molecule. The band at 1534 cm^{-1} is due to the ν (N=O) vibration of the bidentate nitrato species: [19]

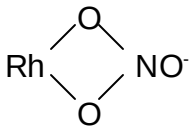

This species was also observed on the NO adsorbed Rh/SiO_2 catalyst by Srinivas et al.[20] The weaker band at 1634 cm^{-1} may be assigned to NO_2 adsorbed on Rh sites.[7,20] NO was also adsorbed on a reduced sample. Rh-Al-MCM-41 was reduced by H_2 at 350 ^oC for 10 min

followed by purging with He for 15 min. NO was then adsorbed at 250 ^{o}C for 10 min. The Rh-NO^{+} band was stronger and appeared at a lower wavenumbers (1895 cm^{-1}) as compared to that on the oxidized sample (Fig. 2b), indicating that more Rh^{+} sites were produced on the reduced catalyst. In addition, two weak bands were seen at 1776 and 1644 cm^{-1}. The 1776 cm^{-1} band can be assigned to Rh-NO^{-}.[20-23] The NO^{-} species with a weakened N-O bond would be easier to dissociate. It is known that NO molecules could be decomposed to N and O atoms on reduced Rh sites and thus oxidize the Rh sites.[21] While the assignment of the band at 1644 cm^{-1} is complicated, Xin et al. [10] and Tanaka et al. [23] assigned the band around 1657 cm^{-1} on Pt catalyst to ν(ONO), but the wavenumbers of nitrito complexes generally fall in the range of 1485-1400 cm^{-1} and 1110-1050 cm^{-1}, as shown by Nakamoto.[22] Therefore this band could also be due to Rh-NO^{-} at different sites on the Rh catalyst , as suggested by Srinivas et al. [20] The IR spectrum of NO+O_2/He adsorbed on Rh-Al-MCM-41 was similar to that of NO adsorbed on the oxidized sample, i.e., Rh-NO^{+} (1904 cm^{-1}), Rh-NO_2 (1634 cm^{-1}) and a bidentate nitrato species (1541 cm^{-1}) were observed (Fig. 2c). When Rh-Al-MCM-41 was treated in a flow of NO_2/He, Rh-NO^{+} (1910 cm^{-1}), Rh-NO_2 (1627 and 1602 cm^{-1}) and a bidentate nitrato species (1554 cm^{-1}) were formed, with Rh-NO_2 as the dominant species (Fig.

2d). The formation of $Rh\text{-}NO^+$ indicates that NO_2 molecules were partly decomposed to NO molecules on Rh sites.

IR Spectra of adsorbed $NO+O_2$ at Different Temperatures. Fig. 3 shows a series of spectra of Rh-Al-MCM-41 in flowing $NO+O_2$/He at different temperatures. After the sample was treated by $NO+O_2$/He at 100 ^oC for 10 min, $Rh\text{-}NO^+$ (1910 cm^{-1}), $Rh\text{-}NO_2$ (1634 cm^{-1}) and bidentate nitrato species (1543 cm^{-1}) were formed (Fig. 3a). In addition, a small peak was observed at 1315 cm^{-1}. This peak was also seen on the NO_2 adsorbed Rh-Al-MCM-41, but not observed on the NO adsorbed sample that was pretreated by H_2. This peak was most likely due to adsorbed NO_2^- species.[22] This species disappeared at 200 ^oC (Fig. 3b). With an increase in temperature, the $Rh\text{-}NO^+$ band (1910 cm^{-1}) grew to a maximum intensity at 250 ^oC, and then declined at higher temperatures. $Rh\text{-}NO^+$ was the dominant species at temperatures below 300 ^oC. By comparison, increasing the temperature from 100 to 350 ^oC resulted in an increase in the bidentate nitrato species (1543 cm^{-1}), but a decrease in the $Rh\text{-}NO_2$ species (1634 cm^{-1}) (Fig. 3). The bidentate nitrato species became the dominant adspecies at 350 ^oC due to oxidation of rhodium. Because NO molecules are easily decomposed to N and O atoms and thus oxidizing the pre-reduced Rh sites to form $[Rh(O_2)^-]$,

other NO molecules can adsorb on the oxidized Rh sites [$Rh(O_2)^-$] to form RhO_2NO, i.e., bidentate nitrato species. At high temperatures, most of the Rh surface was covered by oxygen atoms, and many Rh sites were oxidized to [$Rh(O_2)^-$] sites, so bidentate nitrato became the dominant species.

IR Spectra of Rh-Al-MCM-41 in a Flow of $C_3H_6+O_2$/He. When Rh-Al-MCM-41 was exposed to flowing $C_3H_6+O_2$/He at 100 ^oC, a series of IR bands were observed (Fig. 4a). The weak peaks between 3084 and 2924 cm^{-1} resulted from asymmetric or symmetric C-H stretching vibrations of $=CH_2$ and $-CH_3$ groups of gaseous or weakly adsorbed C_3H_6.[24,25] They disappeared after the sample was purged by He for 15 min. The stronger bands at 1675 and 1430 cm^{-1} can be assigned to acrolein and carboxylate adspecies, respectively.[21,24-26] The appearance of the band at 1594 cm^{-1} indicates the formation of polyene species.[21] The shoulders at 1490 and 1372 cm^{-1} are due to π-allyl complex (π-C_3H_5) and allylic species, respectively.[21,26] The assignments of these bands are summarized in Table 2. These results indicate that oxidation of C_3H_6 took place on the Rh-Al-MCM-41 catalyst at 100 ^oC. With an increase in temperature, the intensity of the carboxylate species (1430 cm^{-1}) grew to a maximum at 250 ^oC and then declined, and it disappeared completely at 350 ^oC. The other adspecies,

i.e., allylic, π-C_3H_5, polyene and acrolein, decreased with the increase in temperature and vanished at 300 ^oC. Moreover, four new bands at 2363, 2335, 2103 and 2046 cm^{-1} appeared at 200 ^oC (Fig. 4b). The bands at 2363 and 2335 cm^{-1} can be assigned to gaseous or weakly adsorbed CO_2 species, while the other two bands are attributed to carbon monoxide adsorbed linearly on two different rhodium sites.[20,21] Increasing temperature resulted in an increase of CO_2 bands but a decrease of CO adspecies bands. The oxidation reaction of propylene has been intensively studied on various catalysts and the mechanism is understood.[21] The above results suggests that the reaction route between C_3H_6 and O_2 on the Rh-Al-MCM-41 catalyst is in agreement with the previous mechanism, i.e., propylene molecules are first adsorbed on the active sites (Rh sites) to produce allylic and π-C_3H_5 species, which can further dehydrogenate to form a polyene species or react with oxygen species to produce acrolein and carboxylate species. They are finally oxidized to CO and CO_2 by oxygen.

IR Spectra of Reaction Between C_3H_6 and NO_x Adspecies. Rh-Al-MCM-41 was first treated with $NO+O_2$/He followed by He purge at 250 ^oC. C_3H_6/He was then introduced and the IR spectra were recorded as a function of time (Fig. 5). As noted above, Rh-NO^+ (1898 cm^{-1}), Rh-NO_2 (1629 cm^{-1}) and bidentate nitrato species (1536 cm^{-1}) were formed after

Rh-Al-MCM-41 was treated with $NO+O_2$/He (Fig. 5a) and their IR bands did not decrease in flowing He for 5 min. After C_3H_6/He was passed over the sample for 15 seconds, the bands due to Rh-NO^+ (1898 cm^{-1}) and bidentate nitrato species (1536 cm^{-1}) declined rapidly, while CO_2 (2363 and 2335 cm^{-1}) and Rh-CO (2025 cm^{-1})[20,21] species were formed (Fig. 5b). In addition, a new weak band at 2174 cm^{-1} was also observed, suggesting the formation of an isocyanate complex (Rh-NCO).[7,20,21,27-29] The Rh-NCO species was detected by many researchers when investigating the interaction of NO and CO on supported rhodium catalysts. For example, Hecker and Bell[27,28] studied the formation of -NCO by *in situ* IR spectroscopy on Rh/SiO_2. They assigned the band at 2300 cm^{-1} to Si-NCO and that at 2190-2170 cm^{-1} to Rh-NCO based on a comparison with the spectra of isocyanate complex over transition metals. The Rh-NCO species at 2172 cm^{-1} was also identified by isotope exchange experiment.[29] The decrease of the IR bands due to Rh-NO^+ and bidentate nitrato species as well as the formation of CO_2, Rh-CO and Rh-NCO species clearly indicated that C_3H_6 reacted with these nitrogen oxides adspecies. Decrease of the 1629 cm^{-1} band was not apparent. This is probably due to the fact that the product H_2O, resulting from oxidation of propylene, also has an IR band near 1629 cm^{-1}. The bands at 1629 and 1536 cm^{-1} vanished in 30 seconds (Fig. 5c). After the sample was treated in a flow of C_3H_6/He for 60 seconds, the Rh-NO^+ and Rh-NCO bands

also disappeared and the CO adspecies became dominant on the surface, with a linear CO band at 2004 cm^{-1} and a bridged CO band at 1830 cm^{-1}.[20]

IR Spectra of Reaction Between $C_3H_6+O_2$ and Adsorbed NO_x. Figure 6 shows the IR spectra observed during the reaction between $C_3H_6+O_2$/He and nitrogen oxides adspecies at 250 ^oC. As $C_3H_6+O_2$/He was passed over the $NO+O_2$ adsorbed Rh-Al-MCM-41, there was a gradual decrease in the Rh-NO^+ band (1898 cm^{-1}) and the bidentate nitrato band (1536 cm^{-1}), and simultaneous formation of CO_2 (2363 and 2335 cm^{-1}). Meanwhile, Rh-NCO (2174 cm^{-1}) and Rh-CO (2103 and 2047 cm^{-1}) were progressively formed. On the other hand, some features that were assigned to acrolein (1670 cm^{-1}), polyene (1594 cm^{-1}), π-C_3H_5 (1492 cm^{-1}) and carboxylate species (1427 cm^{-1}) [21,24-26] also appeared. After 5 min, only a trace of Rh-NO^+ and Rh-NCO were detected, and the other IR features were similar to that of the fresh Rh-Al-MCM-41 catalyst exposed in flowing $C_3H_6+O_2$/He at 250 ^oC (as shown in Fig. 4c). These results indicate that C_3H_6 could also reduce the nitrogen oxides adspecies in the presence of excess oxygen, but the disappearance of nitrogen oxides adspecies required a longer time (> 5 min vs. 1 min) as compared with that in the absence of oxygen (compare Fig. 5 and Fig. 6). This is attributable to the competitive consumption of C_3H_6 by O_2. Besides, CO_2,

not CO, was the main product of propylene oxidation in the reaction between $C_3H_6+O_2$ and nitrogen oxides adspecies.

IR Spectra of Rh-Al-MCM-41 in a Flow of $NO+C_3H_6+O_2$/He. To identify the species present on the catalyst under reaction conditions, IR spectra were recorded in a flow of $NO+C_3H_6+O_2$/He when Rh-Al-MCM-41 was heated from 100 to 350 ^oC. As shown in Fig. 7a, a series of IR bands were observed at 3084-2924, 1899, 1730, 1675, 1635, 1600, 1507, 1428 and 1373 cm^{-1} at 100 ^oC. These bands were also detected on the sample in flowing NO/He, $NO+O_2$/He and $C_3H_6+O_2$/He (Figs. 2, 3 and 4). As indicated above, the weak bands between 3084 and 2924 cm^{-1} are due to the C-H stretching vibration of C_3H_6; the bands at 1899 and 1730 cm^{-1} are attributable to Rh-NO^+ and Rh-NO^- species, respectively. The shoulders at 1675, 1600 cm^{-1} and the weak bands at 1507, 1428 and 1373 cm^{-1} can be assigned to acrolein, polyene, π-C_3H_5, carboxylate and allylic species, respectively.[20-26] The band at 1635 cm^{-1}, assigned to Rh-NO_2 species above, was probably also due to H_2O here because oxidation of C_3H_6 took place at 100 ^oC. When the temperature was raised to 200 ^oC, the IR bands attributed to Rh-NO^+ (1899 cm^{-1}), π-C_3H_5 (1507 cm^{-1}) and carboxylate (1428 cm^{-1}) increased (Fig. 7b). Moreover, two new peaks at 2174 and 1777 cm^{-1} appeared, which

can be assigned to Rh-NCO and Rh-NO^- species, respectively.[20-22,27-29] The formation of Rh-NCO indicates that the reaction between NO and C_3H_6 occurred at 200 ^oC. At 250 ^oC, the IR bands due to CO_2 at 2363 and 2335 cm^{-1} were detected. In addition, a very small peak at 2241 cm^{-1} was also observed, suggesting the formation of gaseous N_2O [20]. The IR bands of these adspecies were changed with an increase in temperature. Rh-NCO and carboxylate species grew to a maximum at 250 ^oC, and then decreased at higher temperatures. The maximum of Rh-NO^+ species appeared at 300 ^oC. At 350 ^oC, besides CO_2, Rh-NO^+ and Rh-NO_2, a new band at 1541 cm^{-1} was detected, which is attributable to the bidentate nitrato species.[19,20] It is noted that propylene was consumed by oxygen and nitric oxide at this temperature. No adsorbed or gaseous CO species was observed during the reaction at 100-350 ^oC.

Reaction Mechanism of NO Reduction by C_3H_6 in the Presence of O_2. As indicated above, when NO was introduced to the oxidized Rh-Al-MCM-41 or NO+O_2 was passed over the reduced sample at 250 ^oC, Rh-NO^+, bidentate nitrato species and a small amount of Rh-NO_2 were observed. Rh-NO^+ was the dominant species on the surface. It was also observed on Rh-Al-MCM-41 in the presence of NO+C_3H_6+O_2/He at 100-350 ^oC (Fig.

7). The nitrogen oxides adspecies were quite reactive towards C_3H_6 at 250 ^oC in the absence or presence of excess oxygen, leading to the formation of Rh-NCO, CO and CO_2 (Figs. 5, 6). However, under reaction conditions, the bidentate nitrato species was not detected until C_3H_6 was totally consumed at 350 ^oC (Fig. 7). It can not be a reaction intermediate in the SCR reaction. It is also unclear if Rh-NO_2 species existed on the catalyst under reaction conditions due to its overlap with the H_2O band. Considering that the concentration of Rh-NO_2 was always much lower than that of Rh-NO^+ on the NO adsorbed Rh-Al-MCM-41 catalyst (Figs. 2,3), its contribution to the production of N_2 and N_2O would be small as compared with that by Rh-NO^+, even if it is formed under reaction conditions. Therefore, Rh-NO^+ may be the main primary intermediate species for the reduction of NO by C_3H_6.

When C_3H_6 and C_3H_6+O_2 reacted with the nitrogen oxides adspecies on the Rh-Al-MCM-41 catalyst, Rh-NCO was produced (Fig. 5 and 6). This species was also observed on the catalyst under reaction conditions (Fig. 7). In the study of NO + CO reaction, Rh-NCO was detected on the rhodium doped catalysts and attracted considerable interests.[19] It was considered to be formed from the reaction between CO and Rh-N resulting from the dissociation of NO on the reduced Rh sites. However, in the SCR reaction, we did not detect any gaseous or adsorbed CO species on Rh-Al-MCM-41 (Fig. 7). Hence the Rh-NCO

species was most probably formed from reduction of Rh-NO^+ by C_3H_6. The Rh-NCO species was reported to be active in reacting with O_2 and NO to form N_2 and N_2O on the Rh/Al_2O_3 catalyst.[30] Rh-NCO may also be another intermediate during the SCR reaction.

As $NO+C_3H_6+O_2$/He was passed over Rh-Al-MCM-41 at 100 ^oC, besides Rh-NO^+ and Rh-NO^- , acrolein, polyene, π-C_3H_5, carboxylate and allylic species were formed (Fig. 7). This suggests that partial oxidization of C_3H_6 took place at 100 ^oC. The reactions between the nitrogen oxides adspecies with propylene took place at above 200 ^oC, as identified by the formation of Rh-NCO, N_2O and CO_2 species. Since the propylene adspecies (polyene, π-C_3H_5, allylic species, etc.) are strong reductants, they can also reduce the nitrogen oxides adspecies at high temperatures. Based on the above results, a possible mechanism for the reduction of NO by C_3H_6 in the presence of excess O_2 on the Rh-Al-MCM-41 catalyst is present as follows:

$$Rh^+ + NO \leftrightarrow Rh\text{-}NO^+ \quad (1)$$

$$C_3H_{6\,(g)} \rightarrow C_3H_{6\,(a)}\ (+[O]) \rightarrow \text{-}C_3H_5,\ \pi\text{-}C_3H_5,\ \text{polyene, ...} \quad (2)$$

$$Rh\text{-}NO^+ + C_3H_{6\,(a)},\ \text{-}C_3H_5,\ \pi\text{-}C_3H_5,\ \text{polyene, ...} \rightarrow \ \text{...} \rightarrow Rh\text{-}NCO \quad (3)$$

$$Rh\text{-}NCO + 1/2\ O_2 \rightarrow \ Rh + 1/2\ N_2 + CO_2 \quad (4)$$

$$Rh\text{-}NCO + NO \rightarrow Rh + N_2 + CO_2 \quad (5)$$

$$NO + 1/2\ O_2 \rightarrow NO_2 \quad (6)$$

$$Rh\text{-}NCO + NO_2 \rightarrow Rh + N_2O + CO_2 \quad (7)$$

$$Rh + 1/4\ O_2 \rightarrow Rh^+ + 1/2\ O^{2-} \quad (8)$$

The reaction begins with the adsorption of NO molecules on the partially oxidized Rh^+ sites to form $Rh\text{-}NO^+$ (reaction 1) and the adsorption of C_3H_6 on the catalyst to form propylene adspecies, such as allylic species, π-C_3H_5, polyene, etc. (reaction 2). The $Rh\text{-}NO^+$ and the adjacent propylene adspecies form the Rh-NCO species (reaction 3). The Rh-NCO then reacts with O_2 , NO and NO_2 to produce N_2, N_2O and CO_2 (reaction 4-7). At the same time, Rh is oxidized back to Rh^+ ions (reaction 8) and thus a catalytic cycle for the SCR reaction is accomplished. Besides the major reaction path, some N_2 and N_2O may also come from NO dissociation because a small amount of $Rh\text{-}NO^-$ species was also observed under reaction conditions (Fig. 7). It is known that reduced Rh metal is active for the decomposition of NO molecules.[21] The above reaction mechanism on the Rh-Al-MCM-41 catalyst is different from that on Pt doped catalysts [8,10,11] as well as Cu-ZSM-5 [1] , Co-ZSM-5 [31] and Mn-ZSM-5 catalysts [32] .

In addition to the SCR reaction, the propylene adspecies can also be oxidized by oxygen. The reaction path is as follows:

$-C_3H_5$, π-C_3H_5 (+[O]) $\rightarrow$ acrolein (+[O]) $\rightarrow$ carboxylate (+[O]) $\rightarrow CO_2$ (9)

$-C_3H_5$, π-C_3H_5 (+[O]) $\rightarrow$ polyene (+[O]) $\rightarrow CO_2$ (10)

The oxidation reaction competes with the SCR reaction for the consumption of propylene.

Conclusions

Rh-Al-MCM-41 was active for the reduction of NO by C_3H_6 in the presence of excess oxygen. The Rh-NO^+ species was observed by *in situ* FT-IR spectroscopy on the catalyst in flowing NO/He, NO+O_2/He and NO+C_3H_6+O_2/He. It could react with propylene and/or propylene adspecies (e.g., π-C_3H_5, polyene, etc.) at 250 ^oC in the presence or absence of oxygen. During the SCR reaction, an isocyanate species (Rh-NCO) was also detected. A main reaction path for the reduction of NO by C_3H_6 was proposed. In this path, Rh-NO^+ and propylene adspecies first form a Rh-NCO species, then the Rh-NCO species reacts with O_2, NO and NO_2 to produce N_2, N_2O and CO_2.

References and Notes

(1) Shelef, M. *Chem. Rev*. **1995**, *95*, 209.

(2) Amiridis, M.D.; Zhang, T.; Farrauto, R.J. *Appl. Catal. B* **1996**, *10*, 203.

(3) Hamada, H.; Kinataichi, Y.; Sasaki, M.; Ito, T. *Appl. Catal*. **1991**, *75*, L1.

(4) Hirabayashi, H.; Yahiro, H.; Mizuno, N.; Iwamoto, M. *Chem. Lett*. **1992**, 2235.

(5) Obuchi, A.; Ohi, A.; Nakamura, M.; Ogata, A.; Mizuno, K.; Ohuchi, H. *Appl. Catal. B* **1993**, *2*, 71.

(6) Iwamoto, M.; Yahiro, H.; Shin, H.K.; Watababe, M.; Guo, J.; Konno, M.; Chikahisa, T.; Murayama, T. *Appl. Catal. B* **1994**, *5*, L1.

(7) Bamwenda, G.R.; Ogata, A.; Obuchi, A.; Oi, J.; Mizuno, K.; Skrzypek, J. *Appl. Catal. B* **1995**, *6*, 311.

(8) Burch, R.; Millington, P.J.; Walker, A.P.; *Appl. Catal. B* **1994**, *4*, 65.

(9) Long, R.Q.; Yang, R.T. *Catal. Lett*. **1998**, *52*, 91.

(10) Xin, M.; Hwang, I.C.; Woo, S.I. *J. Phys. Chem. B* **1997**, *101*, 9005.

(11) Burch, R.; Sullivan, J.A.; Watling, T.C. *Catal. Today* **1998**, *42*, 13.

(12) Naito, S.; Tanimoto, M. *Chem. Lett*. **1993**, 1935.

(13) Kresge, C.T.; Leonowicz, M.E.; Roth, W.J.; Vartuli, J.C.; Beck, J.S. *Nature* **1992**, *359*, 710.

(14) Zhao, X.S.; Lu, G.Q.; Millar, G. J. *Ind. Eng. Chem. Res*. **1996**, *35*, 2075.

(15) Biz, S.; Occelli, M.L. *Catal. Rev.-Sci. Eng*. **1998**, *40*, 329.

(16) Yang, R.T.; Pinnavaia, T.J.; Li, W.; Zhang, W. *J. Catal*. **1997**, *172*, 488.

(17) Borade, R.B.; Clearfield, A. *Catal. Lett*. **1995**, *31*, 267.

(18) Shannon, R.D.; Vedrine, J.C.; Naccache, C.; Lefebvre, F. *J. Catal*. **1984**, *88*, 431.

(19) Arai, H., Tominaga, H. *J. Catal*. **1976**, *43*, 131.

(20) Srinivas, G.; Chuang, S.S.C.; Debnath, S. *J. Catal*. **1994**, *148*, 748.

(21) Matyshak, V.A.; Krylov, O.V. *Catal. Today* **1995**, *25*, 1.

(22) Nakamoto, K. *Infrared and Raman Spectra of Inorganic and Coordination Compounds, Part B*, 5 th ed., Wiley, New York, **1997**; chapter 3.

(23) Tanaka, T.; Okuhara, T.; Misono, M. *Appl. Catal. B* **1994**, *4*, L1.

(24) Gerei, S.V.; Rozhkova, E.V.; Gorokhovatsky, Y.B. *J. Catal*. **1973**, *28*, 341.

(25) Hoost, T.E.; Laframboise, K.A.; Otto, K. *Appl. Catal. B* **1995**, *7*, 79.

(26) Hayes, N.W.; Joyner, R.W.; Shpiro, E.S. *Appl. Catal. B* **1996**, *8*, 343.

(27) Hecker, W.C.; Bell, A.T. *J. Catal*. **1984**, *85*, 389.

(28) Hecker, W.C.; Bell, A.T. *J. Catal*. **1984**, *88*, 288.

(29) Paul, D.K.; McKee, M.L.; Worley, S.D.; Hoffman, N.W.; Ash, D.H.; Gatney, J. *J. Phys. Chem*. **1989**, *93*, 4598.

(30) Bamwenda, G.R.; Obuchi, A.; Ogata, A.; Mizuno, K. *Chem Lett*. **1994**, 2109.

(31) Li, Y.; Slager, T.L.; Armor, J.N. *J. Catal*. **1994**, *150*, 388.

(32) Aylor, A.W.; Lobree, L.J.; Reimer, J.A.; Bell, A.T. *J. Catal*. **1997**, *170*, 390.

Table 1. Catalytic performance of Rh-Al-MCM-41 catalyst for SCR reaction

Temperature	NO Conversion	Selectivity (%)		C_3H_6 Conversion
(^oC)	(%)	N_2	N_2O	(%)
200	5.6	62.5	37.5	2.4
250	34.0	60.3	39.7	43.1
275	68.2	69.0	31.0	100
300	44.9	66.0	34.0	100
325	33.5	65.0	35.0	100
350	23.5	67.0	33.0	100
400	15.8	78.0	22.0	100

Reaction conditions: 0.1 g catalyst, [NO] = [C_3H_6] =1000 ppm, [O_2] = 2%, He = balance and total flow rate = 250 ml/min.

Table 2 Assignments of IR bands for the reaction $C_3H_6+O_2$ on Rh-Al-MCM-41

Bands (cm^{-1})	Assignments	References
3084	ν_{as} (=CH_2), C_3H_6	24, 25
2984	ν_s (=CH_2), C_3H_6	24, 25
2956	ν_{as} (-CH_3), C_3H_6	24, 25
2924	ν_s (-CH_3), C_3H_6	24, 25
2363, 2335	CO_2	20
2103, 2046	ν (CO), CO adsorbed on different Rh sites	20, 21
1675	ν_{as} (C=O), Acrolein	24-26
1594	Polyene species	21
1490-1510	π-allyl complex (π-C_3H_5)	21
1430	Surface carboxylate species	21
1372	Allylic species	26

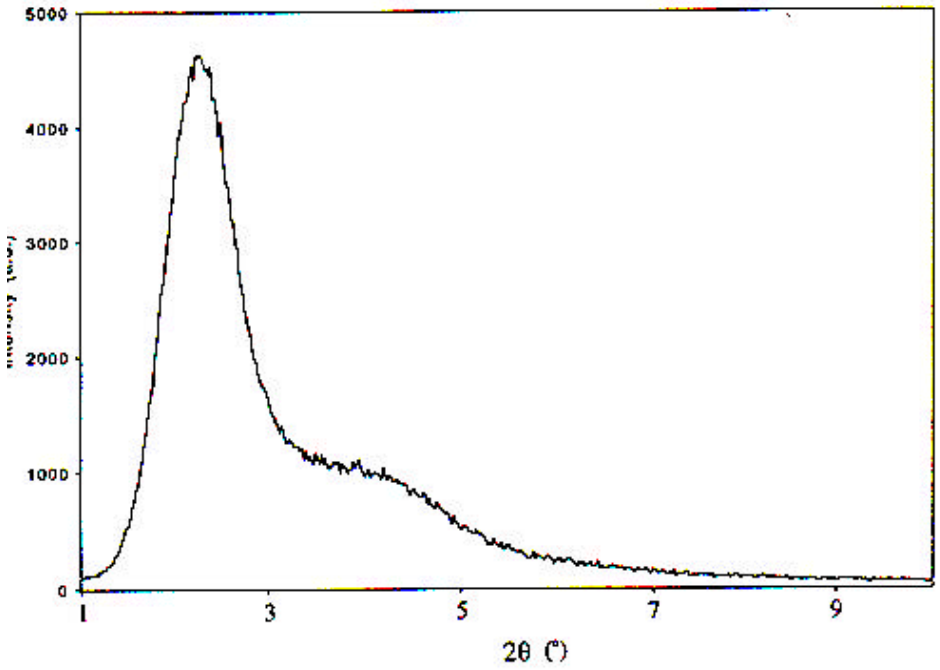

Fig. 1 XRD pattern of Al-MCM-41 sample.

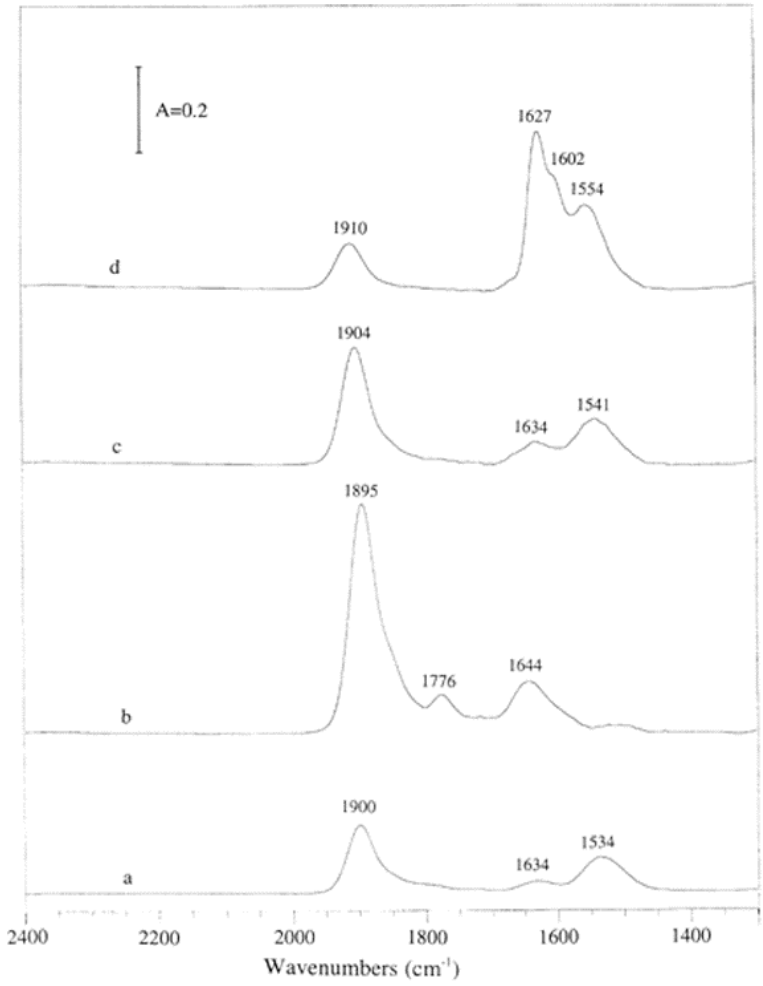

Fig. 2 IR spectra of (a) 1000 ppm NO adsorbed on Rh-Al-MCM-41 pretreated by O_2, (b) 1000 ppm NO adsorbed on Rh-Al-MCM-41 pretreated by H_2, (c) 1000 ppm NO + 2% O_2 adsorbed on Rh-Al-MCM-41 pretreated by H_2 and (d) 1000 ppm NO_2 adsorbed on Rh-Al-

MCM-41 pretreated by H_2. The spectra (100 scans) were collected after the gases were passed over the sample for 10 min at 250 ^oC.

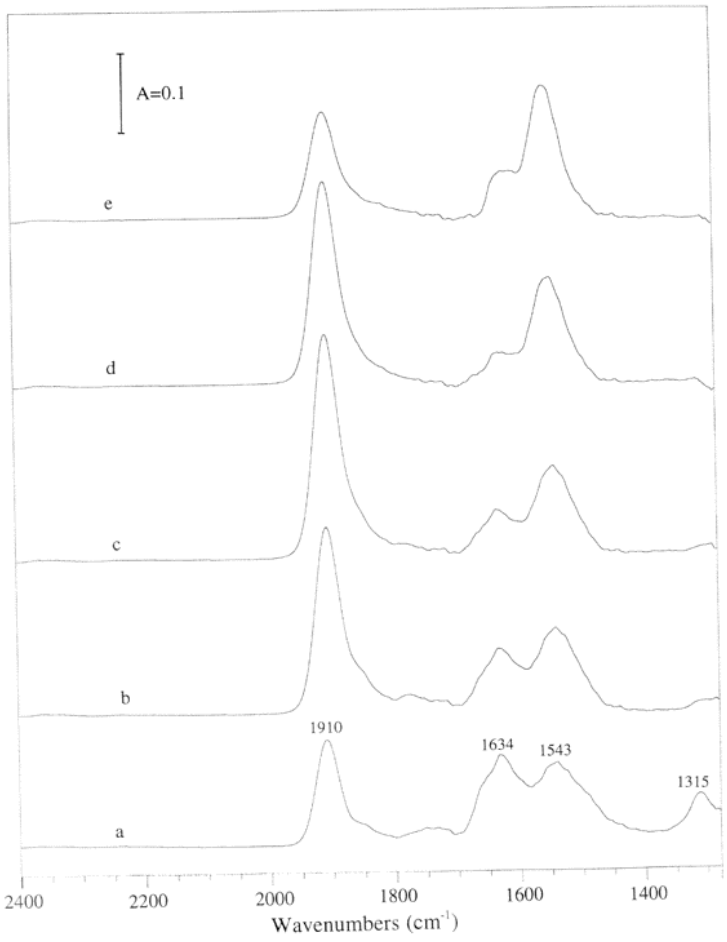

Fig. 3 IR spectra (100 scans) of Rh-Al-MCM-41 in a flow of 1000 ppm NO + 2% O_2/He at (a) 100, (b) 200, (c) 250, (d) 300 and (e) 350 ^oC.

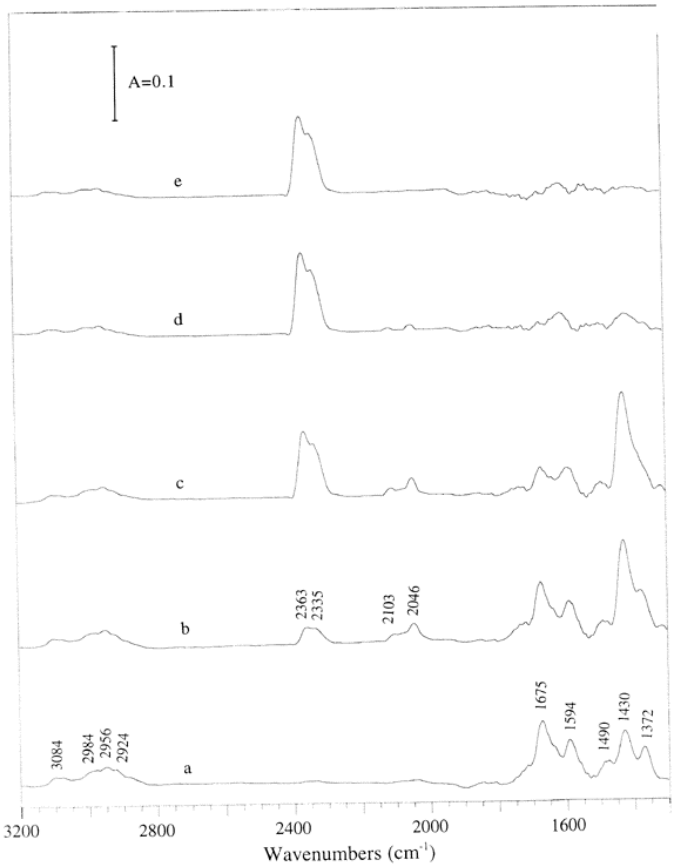
A=0.1
e
d
c
b
a
3084
2984
2956
2924
2363
2335
2103
2046
1675
1594
1490
1430
1372
3200
2800
2400
2000
1600
Wavenumbers (cm-1)

Fig. 4 IR spectra (100 scans) of Rh-Al-MCM-41 in a flow of 1000 ppm C_3H_6 + 2% O_2/He at (a) 100, (b) 200, (c) 250, (d) 300 and (e) 350 ^oC.

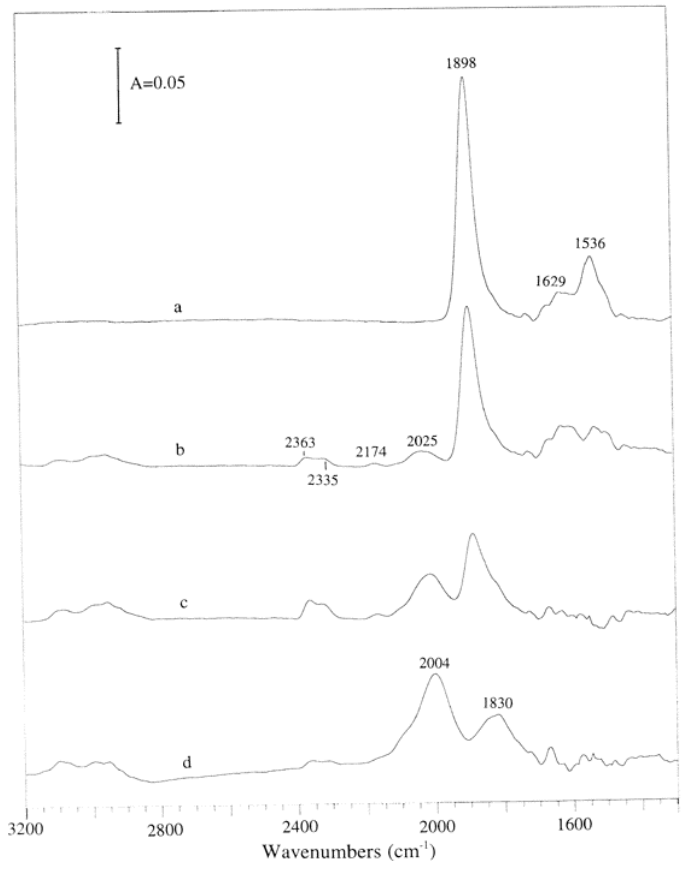

Fig. 5 IR spectra (8 scans) taken at 250 ^{o}C upon passing 1000 ppm C_3H_6/He over the $NO+O_2$ presorbed on Rh-Al-MCM-41 for (a) 0, (b) 15, (c) 30 and (d) 60 seconds.

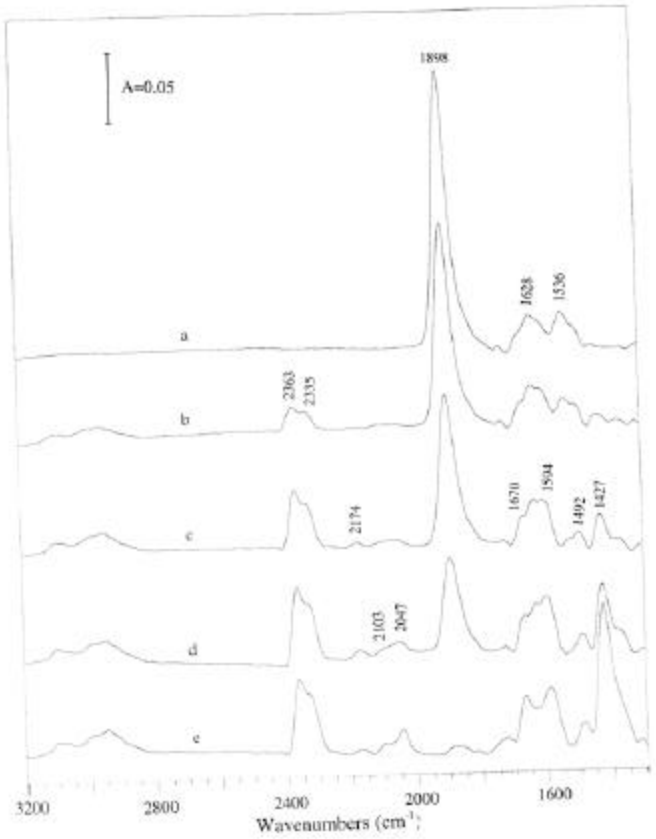

Fig. 6 IR spectra (8 scans) taken at 250 ^{o}C upon passing 1000 ppm C_3H_6 + 2% O_2/He over the NO+O_2 presorbed on Rh-Al-MCM-41 for (a) 0, (b) 15, (c) 30, (d) 60 and (e) 300 seconds.

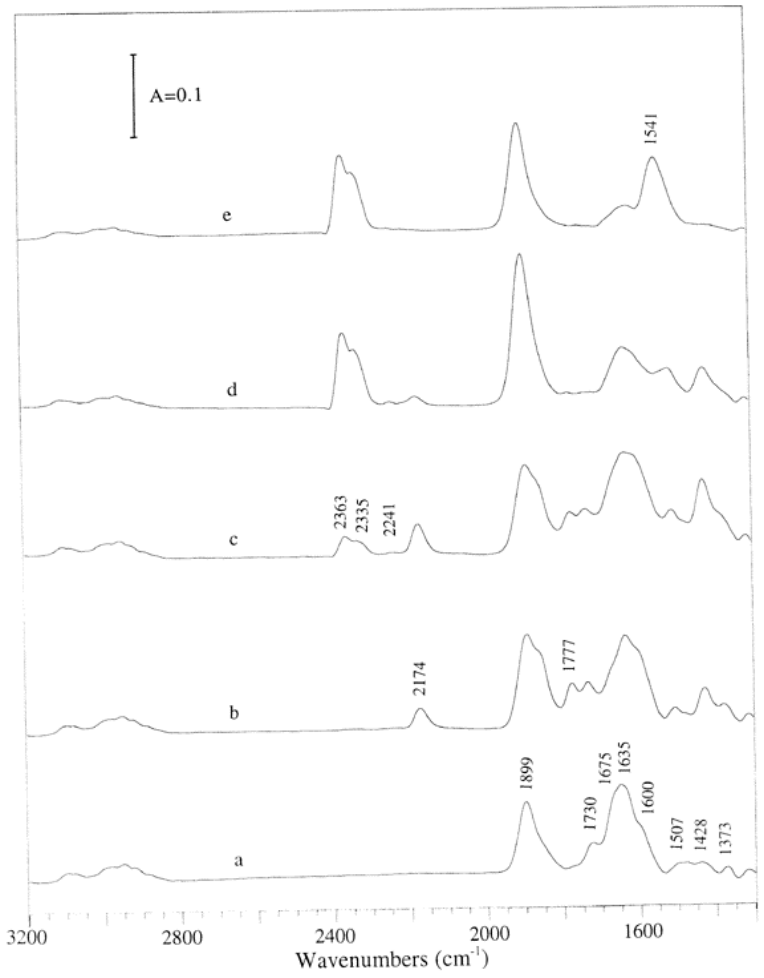

Fig. 7 IR spectra (100 scans) of Rh-Al-MCM-41 in a flow of 1000 ppm NO + 1000 ppm C_3H_6 + 2% O_2/He at (a) 100, (b) 200, (c) 250, (d) 300 and (e) 350 ^oC.

CONCLUSION

Selective catalytic reduction (SCR) of NO by hydrocarbons is investigated on ion-exchanged pillared clays and MCM-41 catalysts, i.e., Cu-TiO_2-PILC, Cu-Al_2O_3-PILC, Cu-ZrO_2-PILC, Cu-Al_2O_3-Laponite, Fe-TiO_2-PILC, Ce-TiO_2-PILC, Co-TiO_2-PILC, Ag-TiO_2-PILC, Ga-TiO_2-PILC, Cu-Al-MCM-41, Ce-Cu-Al-MCM-41, Pt/MCM-41 and Rh-Al-MCM-41. All Cu^{2+}-exchanged pillared clays showed higher SCR activities than Cu-ZSM-5 reported in the literature. Cu-TiO_2-PILC showed the highest activities for SCR of NO than the other cation-exchanged pillared clay catalysts, with 100% of product selectivity for N_2. The catalytic activity increased with copper content until it reached 245% ion-exchange. In particular, H_2O and SO_2 only slightly deactivated the SCR activity of Cu-TiO_2-PILC, whereas severe deactivation was observed for Cu-ZSM-5. Moreover, the addition of 0.5 wt.% CeO_2 onto Cu-TiO_2-PILC increased the activities by about 10-30% while 1.0 wt.% of CeO_2 decreased the activity of Cu-TiO_2-PILC due to pore plugging. Ce-Al-MCM-41 showed little activity, but Cu-Al-MCM-41 and Ce-Cu-Al-MCM-41 were found to be active in this reaction. A high NO conversion to N_2, almost the same as Cu-ZSM-5, was obtained on the Ce-Cu-Al-MCM-41 catalyst. Temperature program reduction results indicated that only isolated Cu^{2+} and Cu^{+} ions were detected in the Cu^{2+}-exchanged Al-MCM-41 samples. 0.5-5 wt% Pt/MCM-41 catalysts showed high activities for NO reduction when C_2H_4 or C_3H_6 was used as the reductant . The maximum NO reduction rate reached 4.3 mmol/g·h under the conditions of 1000 ppm NO, 1000 ppm C_3H_6, 2% of O_2 and He as balance. No or little activity was found when CH_4 or C_3H_8 was used. This difference was related to the different

nature of these hydrocarbons. The Pt/MCM-41 catalyst showed a good stability. H_2O and SO_2 did not cause deactivation of the catalyst. MCM-41 provided the highest specific NO reduction rates for Pt as compared with all other supports reported in the literature, i.e., Al_2O_3, SiO_2 and ZSM-5. Rh exchanged Al-MCM-41 showed a high activity in converting NO to N_2 and N_2O at low temperatures for SCR of NO by C_3H_6. *In situ* FT-IR studies indicated that Rh-NO^+ species was formed on the Rh-Al-MCM-41 catalyst in flowing NO/He, NO+O_2/He and NO+C_3H_6+O_2/He at 100-350 ^oC. This species was quite active in reacting with propylene and/or propylene adspecies (e.g., π-C_3H_5, polyene, etc.) at 250 ^oC in the presence/absence of oxygen, leading to the formation of the isocyanate species (Rh-NCO), CO and CO_2. Rh-NCO was also detected under reaction conditions. A possible reaction pathway for reduction of NO by C_3H_6 was proposed. In the SCR reaction, Rh-NO^+ and propylene adspecies react to generate the Rh-NCO species, then Rh-NCO reacts with O_2, NO and NO_2 to produce N_2, N_2O and CO_2. Rh-NO^+ and Rh-NCO species are two main intermediates for the SCR reaction on Rh-Al-MCM-41 catalyst.